Fundamentals of interactions of electrons with molecules

John H. Moore
Department of Chemistry and Biochemistry, University of Maryland, College Park, Maryland, USA

Petra Swiderek
Institute for Applied and Physical Chemistry, University of Bremen, Leobener Straße / NW2, 28334 Bremen, Germany

Stefan Matejcik
Department of Experimental Physics, Comenius Unversity, Mlynska dolina F2, 84248 Bratislava, Slovakia

Michael Allan
Department of Chemistry, University of Fribourg, chemin du Musée 9, CH-1700 Fribourg, Switzerland
(Dated: July 26, 2009)

I. INTRODUCTION

The electron-molecule processes considered here are:

$e^-(E_i) + AB \rightarrow AB + e^-(E_i)$	elastic scattering	(1)
$e^-(E_i) + AB \rightarrow AB(v) + e^-(E_r)$	vibrational excitation (VE)	(2)
$e^-(E_i) + AB \rightarrow AB^* + e^-(E_r)$	electronic excitation (EE)	(3)
$e^- + AB \rightarrow A^\bullet + B^-$	dissociative electron attachment (DEA)	(4)
$e^- + AB \rightarrow A^\bullet + B^\bullet + e^-$	neutral dissociation (ND)	(5)
$e^- + AB \rightarrow A^\bullet + B^+ + 2e^-$	dissociative ionization (DI)	(6)
$e^- + AB \rightarrow A^\bullet + B^+ + 2e^-$	bipolar dissociation (ion pair formation) (BD)	(7)

Rotational excitation is not explicitly listed, the elastic and inelastic cross sections are meant to be integrated over rotational transitions.

The knowledge of the absolute cross sections for these process in the gas phase is useful not only for the understanding of gaseous plasmas [1], but also as a starting point for the understanding of dense media. An example of the latter are the Monte-Carlo simulations of electron interactions with dense CH_4 and H_2O, motivated by the need to understand and to optimize radiotherapy [2–4]. The input of these simulations are the absolute cross sections for the above processes, both as a function of electron energy and of scattering angle. Similar simulations have been also performed for FEBIP, the main topic of the present book [5–7].

Measurement of each of the various processes requires specialized instruments, which are generally not all present in one laboratory. Different instruments are further often needed to cover different energy ranges.

A great body of existing measurements were performed with the aim of better understanding the resonant phenomena in the collisions. They often cover the energy range of about 0.1-30 eV and emphasize high resolution. They are carried out with instruments using thermionic electron sources and hemispherical or trochoidal electron energy selectors.

A second class of measurements covers the very low energy region, 1-200 meV, with an extremely high resolution and relies on photoelectron sources [8]. This regime is important for the application because the cross section, because every electron in the dense media, including the many secondary electrons, will finally be slowed down to these energies, and because the cross sections, in particular for DEA (eq. 4), can be extremely large at these low energies.

Finally, both for the medical applications and for FEBIP, cross sections are needed also at high energies, about 30-1000 eV. These measurements generally require a different instrument, which does not need high resolution but emphasizes on high sensitivity, required by the low values of

the cross sections at high energies, and also address other specific problems, like the danger of 'polluting' the incident high energy electron beam with slower electrons resulting from inelastic collisions with the metallic apertures. Such slower electrons can seriously distort the data because of the much larger cross sections at low energies. The emerging medical applications led to the construction of new instruments, and recent measurements of data in this high energy regime, particularly by García and coworkers [9].

An important issue is that it is much easier to measure relative cross sections, the shapes of the spectra, and a substantial body of literature on such spectra exists. While the relative data are useful for unraveling the (resonant) mechanism of the processes, they are not useful for simulations and will generally not be covered here.

Another important issue is that it is experimentally much easier to detect charged particles, electrons and positive or negative ions, than to detect neutral products from the electron-molecule collisions. Whereas in the cases of DEA and DI (eqs. (4) and (6) above) the detected charged particle allows conclusions on the cross section for the complementary neutral fragment, in the very important class of ND (eq. (5)) the detection of the neutral particle is a prerequisite for measuring the cross section. Such measurements are consequently generally neglected, very rare and valuable, and we shall devote the Section IV to them. Neutral products are also detected, by thermal desorption, in the condensed phase experiments described in Sec. VI.

As a result, complete sets of cross sections, covering all the above processes and the entire energy range, are extremely rare. Moreover, the choice of the targets was influenced in the past by the prospective applications in plasmas for electronics manufacture and does not include metalorganic compounds relevant for FEBIP. An example are the cross sections for CF_4 given in the book of Christophorou and Olthoff, ref. [1], and reproduced in Fig. 1. Even this set is not 'full' in the sense that it does not contain the angular distributions, required for detailed simulations.

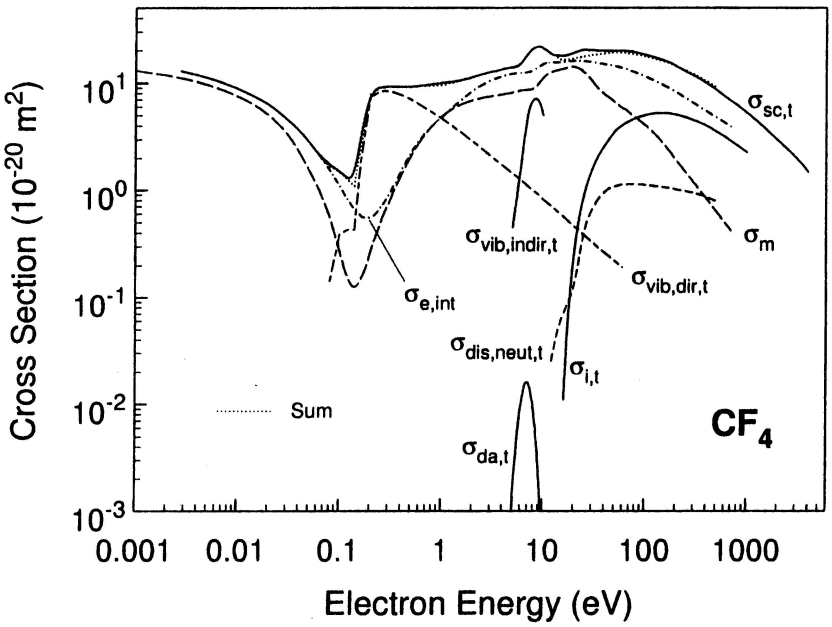

FIG. 1: A complete set of integral cross sections for CF_4. Total scattering: $\sigma_{\mathrm{sc,t}}$; elastic cross section: $\sigma_{\mathrm{e,int}}$; vibrational excitation: $\sigma_{\mathrm{vib,dir,t}}$ and $\sigma_{\mathrm{vib,indir,t}}$; ionization: $\sigma_{\mathrm{i,t}}$; neutral dissociation: $\sigma_{\mathrm{dis,neut,t}}$; dissociative electron attachment: $\sigma_{\mathrm{da,t}}$; momentum transfer: σ_{m}.

Apart from the experiments, the progress of theory is very important because many relevant cross sections, those involving transient molecules (like CF_2), and vibrationally and electronically excited molecules, are very hard or impossible to measure, and we depend on theory to obtain them. The present chapter will therefore present comparisons between experiment and theory whenever available.

This chapter provides a brief overview of the subjects mentioned above, with few illustrative examples. It is organized according to the fundamental processes, approximately in the order

given by the eqs. (1 - 7). It is, necessarily, to a certain degree divided according to the techniques used to measure the cross sections. There is a certain unavoidable 'cross-linking' between the sections, given by the fact that certain processes, in particular DEA and DI, yield both a neutral and a charged fragments.

Section II describes electron scattering processes which do not immediately lead to a chemical change of the target molecule, that is, elastic scattering, and vibrational and electronic excitation. All are important – elastic scattering changes the direction of the electron and is thus responsible for the widening of the incident beam by repeated collisions in dense media. Vibrational excitation slows the electrons down and heats the target. Electronic excitation is an important initial step leading to neutral dissociation (5) and also a means of energy deposition.

Section III describes the first (in the sense that it has the lowest threshold energy) process leading to chemical change, the dissociative electron attachment (4).

Section IV describes the measurements which detect neutral dissociation products, which pose a particular challenge experimentally and are the only means to obtain data on neutral dissociation (5).

Section V concentrates on experiments where positive ions are detected.

Section VI provides a step towards a bridge between the gas-phase cross sections and the applications in the condensed phase. An experiment which provides absolute cross sections for chemical changes in the condensed phase is described, which yields information not only on unimolecular primary processes, but also on the subsequent reactions of the transient species formed initially. The ways in which the resonances and cross sections are influenced by the condensed media are discussed.

Section VII provides a brief summary, conclusions and outlook.

II. ELECTRON SCATTERING

This section will start with a brief description of resonances and then present illustrative examples of measured and theoretical cross sections for elastic scattering and for vibrational and electronic excitation.

A. The role of resonances

At suitable incident energies the electron is often temporarily captured by the target molecule to form a negative ion $\left\{AB^-\right\}_j$, called a resonance, with a lifetime typically in the ps time domain. Despite their short lifetime, resonances often dramatically increase the cross sections for the inelastic processes and for DEA. The processes of vibrational and electronic excitation, and of DEA, are generally dominated by resonances:

$$
\begin{array}{lll}
e^- + AB \rightarrow \left\{AB^-\right\}_j & \rightarrow AB + e^- & \text{elastic scattering} \\
& \rightarrow AB(v) + e^- & \text{VE} \\
& \rightarrow AB^* + e^-(E_r) & \text{EE} \\
& \rightarrow A^{\cdot} + B^- & \text{DEA}
\end{array}
$$

The process is schematically illustrated in Fig. 2. The attachment of an electron transfers the initial wave packet of the nuclei to the resonant potential surface. The surface is usually repulsive in the Franck-Condon region and the nuclei start to separate, to relax. A loss of the electron by fast autodetachment occurs as the nuclei move, the wave packet 'rains down' back onto the potential surface of the neutral molecule. The fast autodetachment leads, by the uncertainty principle, to an energy width Γ of the resonance, which is typically in the 1 meV – 5 eV range.

The system may fall back into the ground vibrational level of the target molecule (elastic scattering); with more relaxation it falls into vibrationally excited levels. DEA results when it 'survives' beyond the 'stabilization point' (curve crossing), R_c. The resulting VE and DEA cross sections are shown (rotated by 90°) on left of the potential curve.

Fig. 3 illustrates, on the example of H_2 [10], several frequently encountered types of resonances. The 'shape resonance' results when an electron is temporarily captured into an normally unoccupied

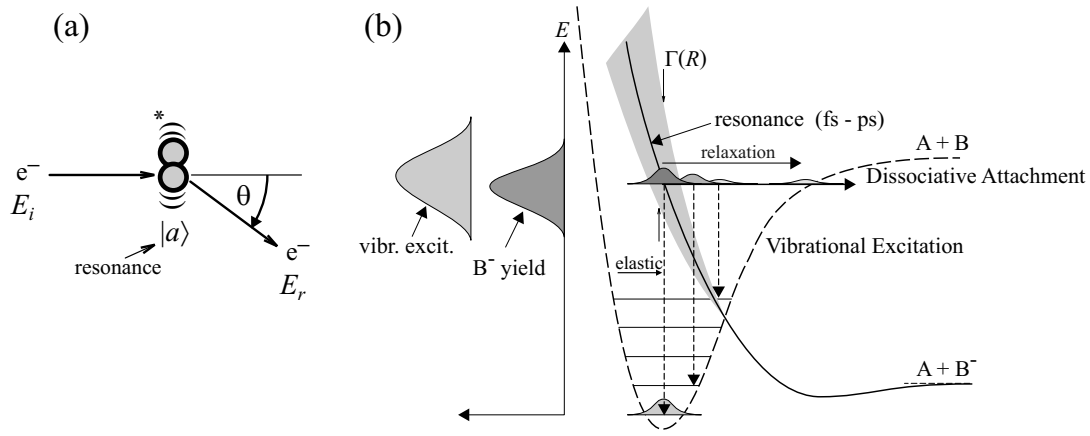

FIG. 2: (a) A schematic diagram of an electron-molecule collision. (b) A schematic diagram of the role of a resonance in the electron collision.

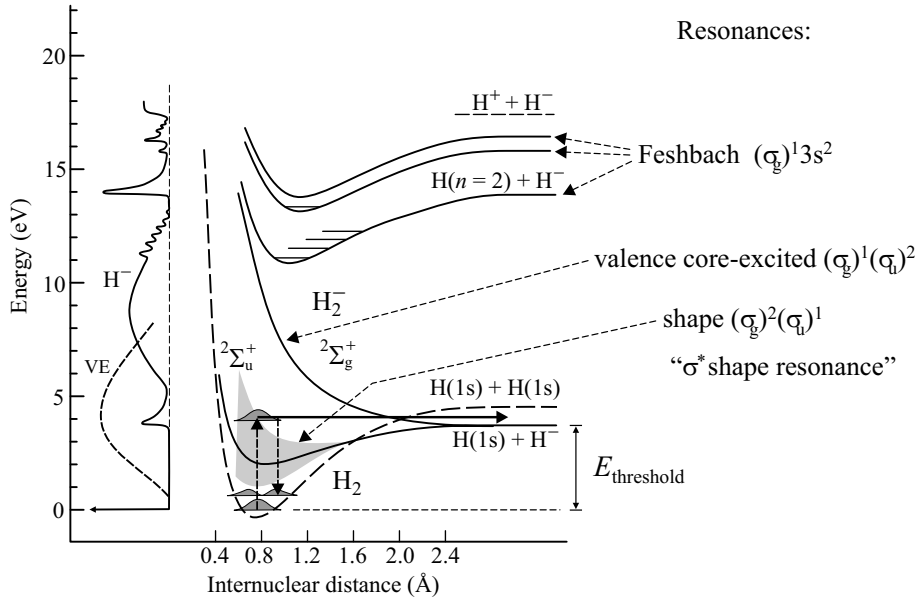

FIG. 3: Schematic diagram of selected resonances in H_2. Schematic VE and DEA (yield of H^-) cross sections are shown (rotated by 90°) on the left of the potential curves.

(virtual) orbital and resides there for a short time because it has to tunnel through a centrifugal barrier in order to leave. In this case it is the σ_u LUMO (lowest unoccupied molecular orbital), the resulting $^2\Sigma_u$ resonance has the configuration $(\sigma_g^2)(\sigma_u)$ and may be called a 'σ^* shape resonance' for short. Its 'parent state' (the state of the neutral target obtained when the 'extra' electron is formally removed) is the electronic ground state of H_2. The width of this resonance in H_2 is more than 2 eV [11] and it consequently gives rise to a very broad band in the VE cross section [12, 13].

Interestingly, the same resonance gives rise to a DEA band which is much narrower than the band in VE. This is because the DEA band has a vertical onset at the DEA threshold, and, on the high energy side, the DEA cross section falls rapidly because the nuclear wave packet has very little chance to survive when the attachment occurs at low internuclear distance, that is, at higher energy. This illustrates that both the VE and DEA are complementary means of detecting resonances, but one and the same resonance may appear very differently in both channels.

Another noteworthy aspect is that, because of the large autodetachment width and thus very fast autodetachment, the elastic and VE channels 'win' by far (about a factor of 10^5) in the competition

with DEA. This has two important consequences: The DEA cross section is small, 0.16×10^{-24} m^2 [14], and the isotope effect is large – the cross section for D^-/D_2 is about 200× smaller than that for H^-/H_2. This can be easily rationalized qualitatively, the heavier deuterium moves, at the same energy, slower than hydrogen, and thus needs a longer time to reach the stabilization point at R_c, leaving more time for autodetachment. Large isotope effects are not uncommon in DEA by low-lying shape resonances, further examples are CH_3OH, C_2H_5OH [15], and C_2H_2 [16]. This suggests that one may gain insight into the role of DEA in certain application cases by using deuterated precursors.

A repulsive resonance with the configuration $(\sigma_g)(\sigma_u)^2$, called a valence core-excited resonance, and resulting when the incoming excites an electron before being captured in the same valence orbital. The parent state is a valence-excited state of H_2. The term symbol is $^2\Sigma_g^+$ and it can conveniently be written as $^2(\sigma_g, \sigma_u^2)$, meaning that, with respect to the target H_2, the resonance has a hole in the σ_g orbital and an additional double occupation of the σ_u orbital. This resonance causes only little VE because the probability of its formation, being a two-electron process, is quite low in comparison with a shape resonance. But it causes a broad DEA band, because it has a much narrower autodetachment width than the shape resonance and the nuclei thus have a larger probability to reach R_c.

At still higher energies a large number of core-excited resonances with double occupation of Rydberg-like orbitals is found. The lowest can be written as $^2(\sigma_g, 3s^2)$. Its parent state is the $^3(\sigma_g, 3s)$ Rydberg state of H_2, and its 'grandparent state' is the ground state of H_2^+, $^2(\sigma_g)$. The resonance lies about 0.4 eV below its parent Rydberg state and is called a Feshbach resonance because it cannot decay into its parent state. Since the two excited electrons reside in a Rydberg-like orbital, which is spatially diffuse and have little density between the nuclei, they do not strongly contribute to binding and the potential curve of the Feshbach resonance is *a priori* similar to that of the cation, that is, not dissociative. In reality, however, the Feshbach resonances are often predissociated by repulsive (valence) states, and they are responsible for the sharp structures and bands in the 11-18 eV range of the DEA spectrum in Fig. 3. In fact, such predissociations are common among many molecules and Feshbach resonances are a major and very frequent cause of DEA in the 6-15 eV range of electron energies.

Sometimes large cross sections and sharp structure are found at low energies which can not be assigned to any of the above resonance types. Examples are HF (Ref. [17] and references therein), where a narrow threshold peak followed by sharp structures is found in VE, although only a broad shape resonance similar to that of H_2 would be expected. The threshold peak and the structures are assigned to Vibrational Feshbach Resonances (VFR) and are due do dipole and polarizability binding of the incoming electron at elongated interatomic distances. A similar threshold peak and structures are found, for example, in CO_2 [18, 19], where it is ascribed to a 'virtual state'. These 'exotic resonances' near threshold are the subject of considerable interest [20], but it is uncertain whether they are also found in condensed state.

B. Elastic scattering

As already mentioned, elastic scattering changes the direction of the electrons and is thus important in the simulations like those of García and coworkers – it influences how strongly does the incident beam widens in condensed media. The results for tetrahydrofuran (THF, Ref. [21] and references therein) are shown in Fig. 4 as an illustrative example of measured and calculated elastic cross section. Both calculated results were obtained by *ab initio* calculations and the agreement is seen to be satisfactory. Critical are low energies, where target polarization becomes important, and low energies combined with low scattering angles, where the cross section becomes very large due to long-range dipole ($\mu = 1.75$ D for THF) interaction. It should be pointed out, however, that the numerical requirements of this type of calculations are very large and the method is consequently not easily scalable to much larger molecules. An altermative in this respect is the independent-atom method (IAM), employing a quasi-free nonempirical model, which has recently been revised to improve its foundation and accuracy and yields satisfactory results at higher energies, from about 30 eV to a few keV [9].

Preliminary elastic cross sections of a FEBIP-relevant compound, $Pt(PF_3)_4$, are shown in Fig. 5. Additional measurements will be required to obtain a more complete set of cross sections, but already at this stage it is clear that this nearly spherical molecule with many electrons leads

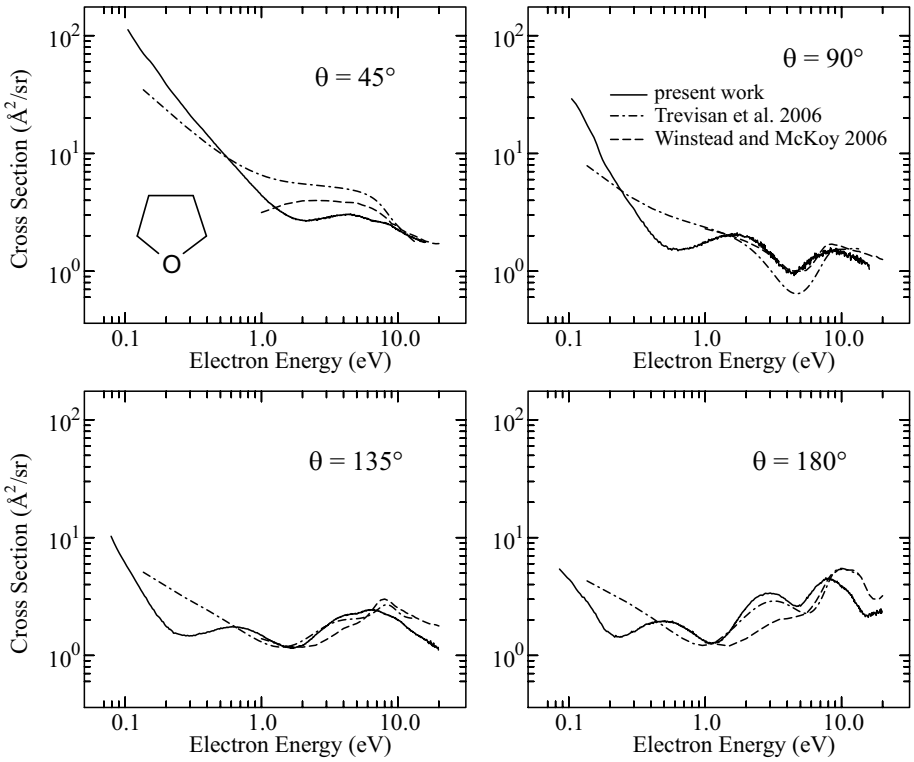

FIG. 4: Elastic cross sections of tetrahydrofurane shown as a function of electron energy at four representative scattering angles [21]. The calculated data of Trevisan *et al.* [22] and of Winstead and McKoy [23] are shown for comparison.

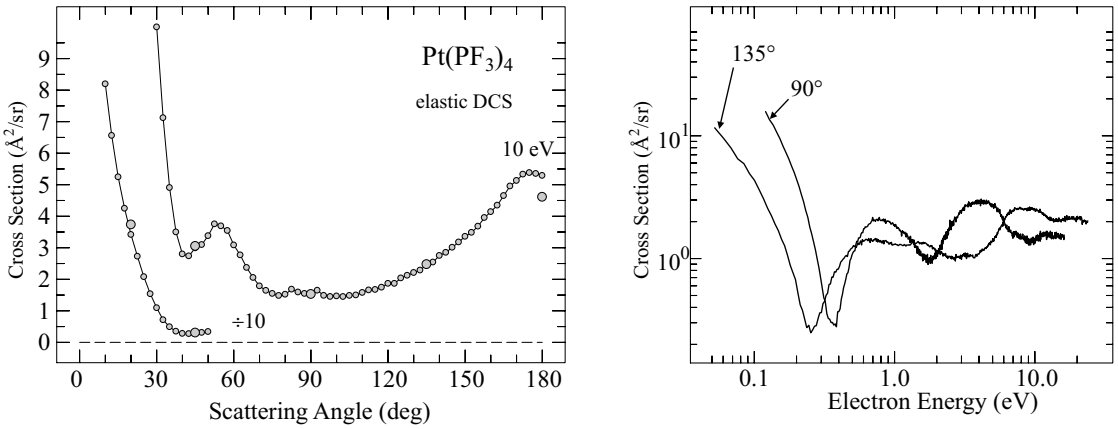

FIG. 5: Elastic cross sections of $Pt(PF_3)_4$ shown as a function of scattering angle at 10 eV on the left, and as a function of electron energy at the scattering angles $\theta = 90°$ and 135° on the right.

to interesting features. The angular distribution is unusual in the sense that it has a narrow minimum around 40°. Deep Ramsauer-Townsend minima appear in the energy-dependence of the cross section.

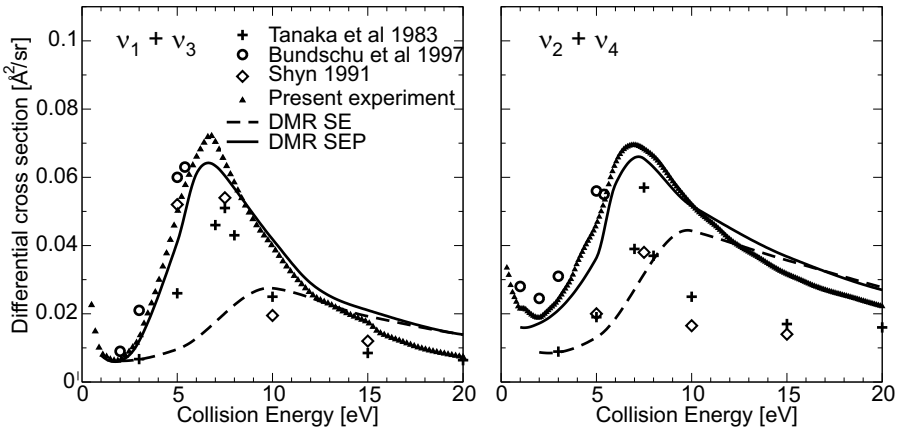

FIG. 6: Cross sections for vibrational excitation of methane shown as a function of electron energy at the scattering angle $\theta = 90^\circ$ (from ref. [24]). The experimental results from Fribourg are shown by triangles, the remaining symbols show earlier experimental data of Tanaka *et al.* Buntschu *et al.* and Shyn. The solid and dashed lines show the results of two levels of theory as explained in the text.

C. Vibrational excitation

The role of vibrational excitation is primarily slowing-down of the electrons and heating the target. The cross sections of methane (THF, Ref. [24] and references therein) are shown in Fig. 6 as an illustrative example. The closely-spaced individual modes can not be resolved, primarily because of the rotational broadening of the vibrational bands, and the sums for $\nu_1 + \nu_3$ (both are C-H stretch vibrations) and $\nu_2 + \nu_4$ (both are H-C-H deformation vibrations) are shown. Methane is also illustrative of the present capacity of theory, as Fig. 6 compares the experiment with the results of calculations carried out using the discrete momentum representation (DMR) method of Čársky and Čurík. This method is also fully *ab initio* and has the advantage of being applicable even to larger, many-modes molecules. It has recently been improved by including the target polarizability (results labeled as SEP, static exchange with polarizability, in Fig. 6), which brings a substantial improvement over the older version without polarizability (results labeled as SE in the Figure) at energies below 10 eV. The agreement of experiment and the SEP theory is very satisfactory.

D. Electronic excitation

Electronic excitation by electron impact has been extensively studied both experimentally and theoretically in atoms, where it is important for lighting applications (for an illustrative example, see Ref. [25] and references therein). Absolute measurements in polyatomic molecules are much more rare, and the corresponding theory is much less advanced.

The electronic excitation of the lowest electronic state in ethene, a prototype of π electronic systems, will be presented here as an illustrative example of the state of experiment and of *ab initio* theory in polyatomic molecules [26].

The results are shown in Fig. 7. For the comparison with theory it is important that the experiment covers the entire angular range from 0° to 180°. The figure also illustrates the problems encountered with *ab initio* calculations. The older version of the theory reproduced well the shapes and overall trends of the cross sections, but overestimated its magnitude, by about a factor of two within the first about 2 eV above threshold. Later it was realized that this discrepancy is due to the neglect of the target polarization, and its inclusion resulted in a great improvement of the magnitude near threshold. But the theoretical effort is substantial, it can not be scaled to much larger molecules, and the theory is useful only within the first about 4 eV above threshold, it fails as more 'final channels', possibilities of the resonances to decay into higher-lying electronic states,

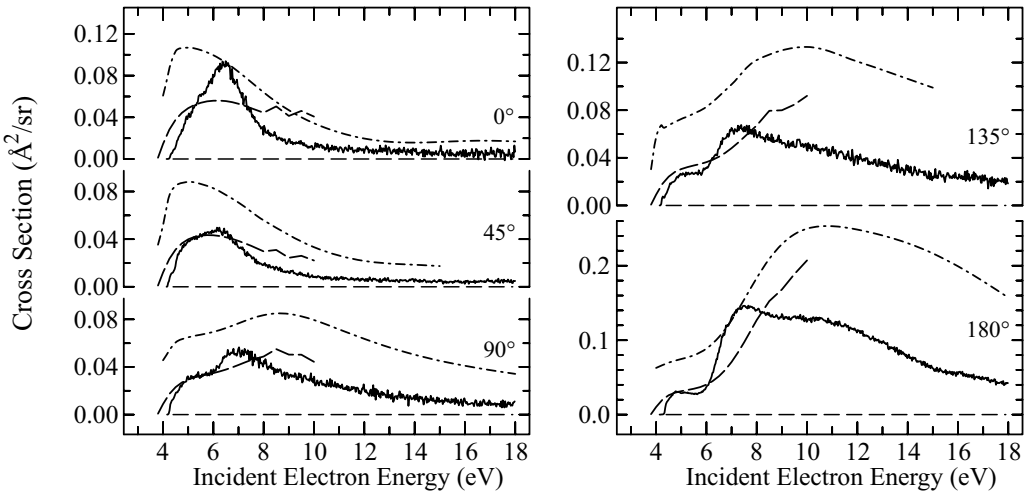

FIG. 7: Cross sections for exciting the $\tilde{a}\ ^3B_{1u}$ triplet state of ethene, summed over all ro-vibrational transitions. Dash-dotted lines show the older calculated results of Sun *et al.* [27], dashed lines the more recent theoretical data [26], which includes target polarization and reproduces better the near threshold region.

open up. It is clear that *ab initio* theory is very useful in the near-threshold energies where more approximate theories fail, but can not provide all the data required for simulations.

For the applications, it is important to know also the cross sections for the excitation of the higher excited states, and to know the cross sections at higher energies (Refs. [2, 4] and references therein). At higher energies, the direct excitation of dipole-allowed transitions becomes dominant and the subsequent fragmentation of the excited states may be the primary mechanism of neutral dissociation.

III. DISSOCIATIVE ELECTRON ATTACHMENT

Dissociative electron attachment cross sections span many orders of magnitude, as can be seen in the overview Fig. 8. In some cases, like the hydro- and fluoro-carbons discussed in Sec. IV, including CF_4 shown in Fig. 1, DEA cross sections are negligible as means of producing reactive intermediates, the radicals. In other cases, in particular at low energies, DEA cross sections may become very large, up to 10^{-15} cm^2. The size of the cross section is to a large degree given by the competition of dissociation with autodetachment. Since autodetachment tends to be slower at low energies, when the electron leaves with little energy, DEA cross sections are larger there than at higher energies, when the autodetachment is faster. This argument is valid for the shape resonances. The Feshbach resonances may have slow autodetachment even at higher energies, 6-15 eV, making the cross sections larger, but not as high as at very low energies, because the probability of forming the Feshbach resonances, a two-electron process, is lower that that for forming the shape resonances.

This section will present few illustrative examples of DEA, intended to show also the progress of theory, and various possibilities of 'control', ways to influence the outcome of the reaction.

A. Diatomic molecules

Measured and calculated DEA spectra of HBr are shown in Fig. 9 as an example where detailed experiment and a very successful calculation are available.

The cross section is fairly large, although one would expect a σ^* shape resonance with a very fast autodetachment like that in H_2, described in Sec. II A, and consequently a small cross section. The large size of the cross section is due to the dipole binding and the ensuing vibrational Feshbach resonances. The larger cross section reveals a more favorable competition with autodetachment,

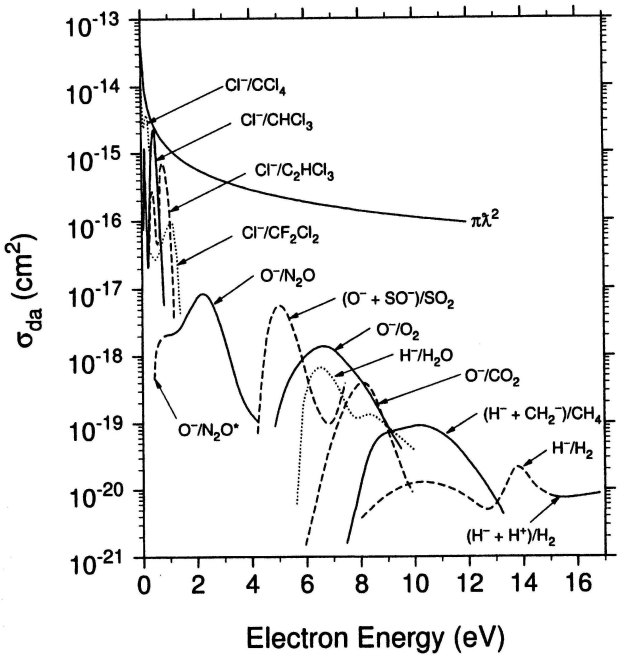

FIG. 8: Dissociative electron attachment cross sections for a number of molecules. From Christophorou *et al.* [1].

confirmed also by the isotope effect, which is seen in Fig. 9 to be about a factor of two, sizeable, but much less than in H_2.

Interesting are the downward steps at the energies of the vibrational levels of HBr. They were first discovered in HCl [31] and are due to 'interchannel coupling': the channel of DEA becomes less populated when the channel of vibrational excitation into a given v opens up.

The threshold phenomena which obviously dominate DEA in this case cannot be described by the 'local' resonance model, where the resonance is described only by ist potential curve and R-dependent width Γ, but a 'nonlocal' resonance model devised by Domcke and coworkers [30], where Γ is also a function of energy, becomes successful. Unfortunately, this model can not be extended to molecules with more than two atoms.

B. Polyatomic molecules: acetylene

Acetylene is mentioned here because it is perhaps the only example where absolute DEA cross section for a more than three-atomic molecule was calculated *ab initio* and the result was validated experimentally. It thus shows the direction for the future.

The absolute cross sections are shown in Fig. 10 (see also Azria and Fiquet-Fayard [32] for an earlier measurement). There is a certain similarity with the spectra of H_2 in Fig. 3. The band at 3 eV has an onset at the thermodynamic threshold and is due to a shape resonance with a temporary electron capture in the π_g orbital. The cross section at this band was successfully calculated by Chourou and Orel [33].

The isotope effect was measured later [16]. It was then realized that the cross section rises rapidly with initial vibrational excitation of the target, that is, with the temperature, and a substantial rise is found already at room temperature. It was necessary to include the temperature dependence to correctly reproduce the isotope effect [34].

The theory provided important insight into the mechanism of the dissociation, which is symmetry-forbidden in the linear geometry. The π^* resonance of acetylene has to bend before it can dissociate. In the bent state the dissociation proceeds without activation barrier, but the necessity to bent makes the dissociation time longer, the competition with autodetachment less favorable, and the DEA cross section small. In fact, the role of DEA in the overall production of

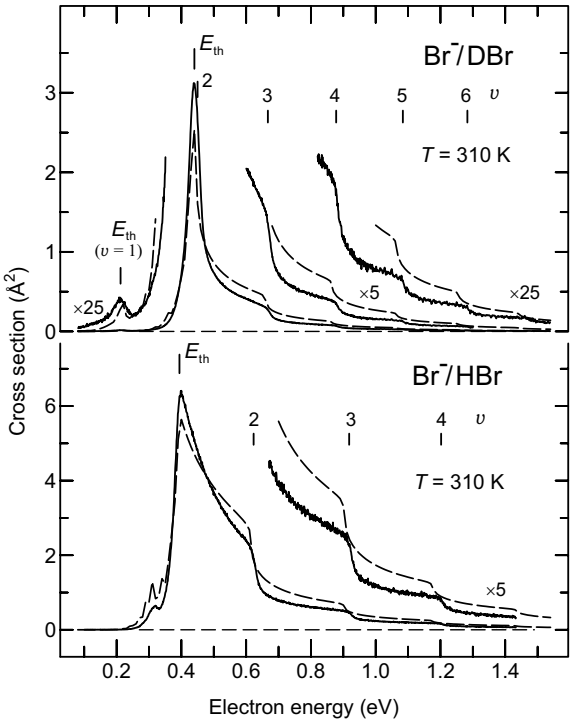

FIG. 9: Solid lines: high resolution (10 meV) absolute cross sections for Br^-/HBr and Br^-/DBr, obtained by normalizing earlier relative spectra [28] to the absolute values measured later [29]. Dashed lines: predictions of the nonlocal resonance theory [28, 30], with the final temperature taken into account, but without convolution with an apparatus function. Note that the experimental and theoretical data sets are independently on absolute scales, without any mutual normalization or scaling! The vibrational thresholds (v) and the DEA thresholds E_{th} are indicated. Reproduced from Ref. [29].

reactive intermediates in acetylene is, like in the case of CF_4 described in Sec. IV below and shown in Fig. 1, presumably very small.

Calculating the cross section for the 8 eV Feshbach resonance remains, however, beyond the capacity of the current theory, although Feshbach resonance-mediated DEA was calculated in a pioneering work for the triatomic molecule H_2O [35, 36].

C. Controlling the outcome of DEA

In DEA it is common that for a given target different resonances, formed at different incident energies, dissociate into different fragments. An example has already been presented in Fig. 10, where C_2H^- was produced at 3 eV and H^- and C_2^- were produced at 8 eV. DEA is in this respect fundamentally different from photochemistry, ruled in most cases by the Kasha's rule, which says that radiationless transitions from higher excited states to the lowest excited state are generally faster than chemical reactions. That means that photochemistry from higher excited states is not different from that of the lowest excited state.

Other examples of selective DEA have recently been observed in molecules of biological relevance, the nucleobases [37]. Another example was reported by Prabhudesai *et al.* who observed, using selective deuteration, that for methanol, ethanol, acetic acid and n-propyl amine H^- is lost from the heteroatom around 6.5 and 7.7 eV, and from the alkyl group around 10 eV [38].

A number of selectivities were observed for alcohols and ethers, for example that Feshbach resonances with core hole on the oxygen lone pair orbitals n or $\bar{n}$ break the O-H bond but not the O-C bond, and this observation was rationalized using potential curves of the parent Rydberg states [39]. A selectivity was even found in cleaving various C-O bonds in asymmetric ethers [40].

Fig. 11 shows an illustrative example of selectivity of the type reported by Prabhudesai *et al.*

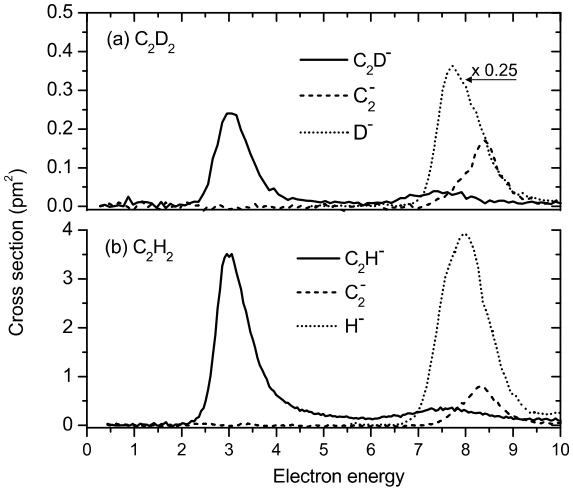

FIG. 10: Dissociative electron attachment cross sections for (a) C_2D_2 and (b) C_2H_2.

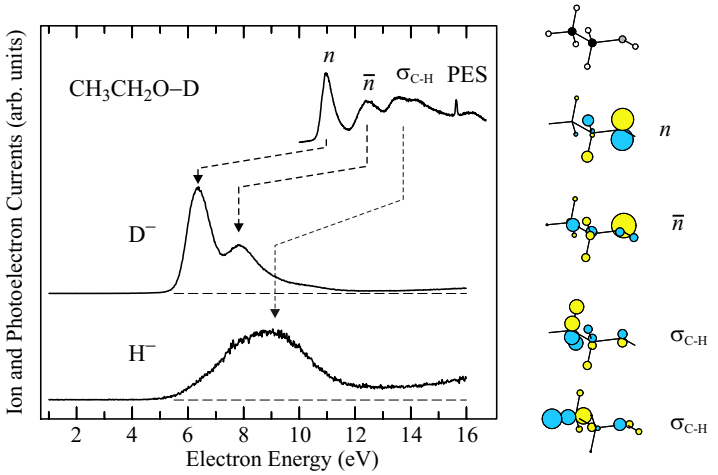

FIG. 11: Dissociative electron attachment (H^- and D^- yields) spectra of partially deuterated ethanol, C_2H_5OD. The photoelectron spectrum shown on the top aids the assignment of the Feshbach resonance bands. Shown on the right are schematic diagrams of the orbitals involved in the cationic states in the photoelectron spectrum and which are only singly occupied in the Feshbach resonances.

[38]. The figure is based on the data of Ref. [15]. The assignment of the DEA bands is aided by comparison with the grandparent states of the cation, revealed by the photoelectron spectrum (PES) on the top of the figure. Since the binding energy of the two $3s$ electrons of the Feshbach resonance with respect to the cation is always about 4.5 eV, the two bands in the D^- yield must be the $^2(n, 3s^2)$ and $^2(\bar{n}, 3s^2)$ Feshbach resonances, where n and $\bar{n}$ are the out-of-plane and the in-plane lone pair orbitals localized predominantly on the oxygen atom, as shown by the orbital diagrams in the figure. D, bound to the O-atom, is thus ejected (as a negative ion) exclusively by resonances where the hole is localized predominantly on the O-atom. The signal around 9 eV in the H^- yield must be due to Feshbach resonances of the type $^2(\sigma, 3s^2)$, with a hole in one of the σ orbitals. H, bound to the C-atom, is thus ejected predominantly by resonances where the hole is localized primarily on the alkyl group.

These selectivities open up, in principle, the possibility of controlling the chemistry by tuning the electron energy. This possibility can presumably not be used in practice, however, because there is not sufficient control over the energies of the secondary electrons in FEBIP, and because this selectivity concerns only DEA, whereas a number of other processes contribute to the production

of reactive intermediates at the same time.

There is a second kind of selectivity whereby fragments in different chemical surroundings have different sensitivities to being dissociated by electrons. An interesting example are halogen atoms, connected to an aromatic ring or to a double bond, either directly or *via* a methylene (-CH_2-) group.

The result may seem surprising at first: although the electron is captured into a π^* orbital, the halogen situated further away from the aromatic ring (or a double bond) is removed preferentially [41, 42].

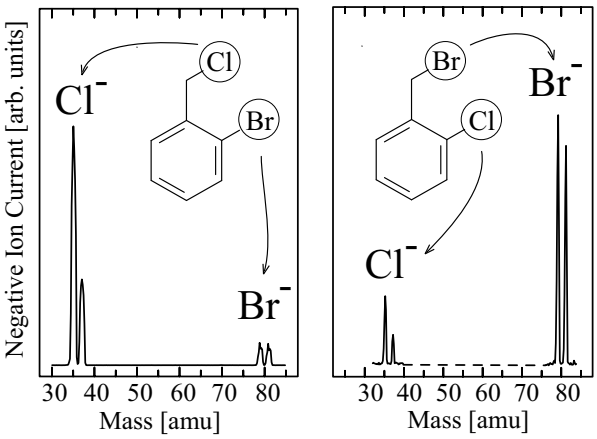

FIG. 12: Dissociative electron attachment cross sections for two halosubstituted toluenes, at an incident energy of about 0.4 eV. The signal of the halogen attached directly to the ring is always weaker.

This opened up the possibility to synthesize dihalo substituted toluenes which lost preferentially Cl^- or Br^- upon the attachment of an electron into the π^* orbital of the benzene ring, as shown in Fig. 12 [43]. The principle is operative also for substituents other than halogen, namely alkoxy [44].

Another way to influence DEA is to choose compounds with 'good leaving groups'. These are generally halogens, where DEA is driven by their large electron affinity. But compounds with very stable neutral fragments, for example phenyl azide which looses N_2 upon attachment of 0-0.5 eV electrons, also have large DEA cross sections [45].

IV. REACTIVE NEUTRAL FRAGMENTS FROM ELECTRON IMPACT FRAGMENTATION

Electron-impact fragmentation of molecules in a gas yields ions and neutrals. The neutrals are in the majority; many of these are chemically reactive. The sticking probability for the neutrals at nearby surfaces is much less than for the ions. In practical situations, in the absence of confining fields, ions may be quickly lost to the walls of an apparatus so that the concentration of neutrals, even highly reactive radicals, can increase by orders of magnitude over that of the ions (see for example ref. [46]).

Three electron-impact fragmentation processes yield neutral species:

neutral dissociation (ND)

$$e^- + AB \rightarrow A + B + e^-,$$

dissociative ionization (DI)

$$e^- + AB \rightarrow A + B^+ + 2e^-,$$

dissociative attachment (DEA)

$$e^- + AB \rightarrow A + B^-,$$

(It is understood in that 'AB' represents in general a polyatomic molecule, and 'A' or 'B' or both represent polyatomic fragments.)

A few broad generalizations will help in understanding the nature of the products of electron-impact fragmentation. From elementary chemistry, recall that, with very few exceptions, stable molecules possess an even number of electrons; stability is derived from having all electrons paired.[156] Neutral dissociation requires the rupture of a chemical bond and the separation of a bonding pair of electrons. It follows that both fragments are odd-electron species. They are *radicals* and tend both to be very reactive. In chemical notation the unpaired electron is explicitly notated. For example, neutral dissociation of CF_4:

$$e^- + CF_4 \rightarrow {}^{\bullet}CF_4 + {}^{\bullet}F + e^-,$$

Dissociative ionization and dissociative attachment rupture a bond and ionize one of the fragments. Stable ions tend to be even-electron species (for example, F^+, F^-, CF_3^+). The neutral fragment of dissociative ionization or dissociative attachment is thus usually a radical.

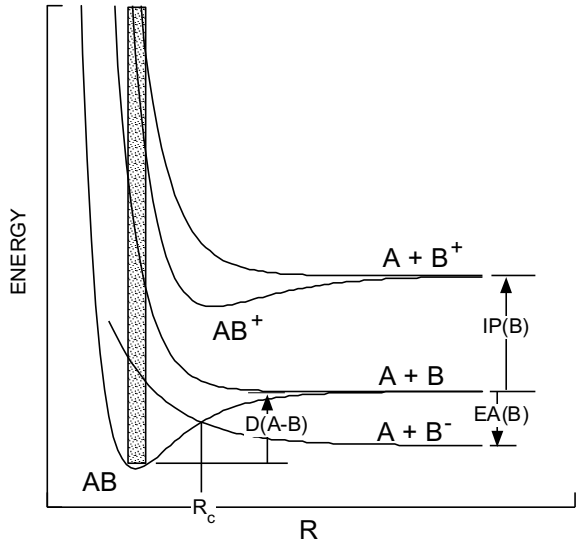

FIG. 13: A potential energy diagram for the polyatomic molecule AB representing a cut through electronic potential energy surfaces along the A-B bond direction. Shown are typical potential energy curves for bound and unbound states of the neutral AB molecule and the AB^+ ion, as well as an unbound state of the negative ion, AB^-. IP(B) is the ionization potential of the B fragment, EA(B) the electron affinity of B, and D(A-B) is the A-B bond energy.

Much can be learned about the process of electron-impact fragmentation from an examination of a generalized potential-energy diagram for the target molecule (Figure 13). (In fact, a many-dimensional energy surface is required to describe each electronic state of a polyatomic molecule. Figure 13 describes a cut through some of these surfaces along the A-B bond direction.) The initial step in electron-impact-induced chemistry involves excitation of the parent to a dissociative electronic state or to a bound state with sufficient excess energy to place the molecule above the dissociation limit. An electronic transition occurs in a brief time compared to the period of vibrational motion in a molecule; the positions of the atomic nuclei are essentially frozen. This is the Franck-Condon approximation. On the potential-energy diagram, electronic excitation is represented as a vertical transition from near the equilibrium confirmation of the parent on the ground electronic state surface to an excited state surface in an unchanged geometry. This so-called "Franck-Condon region" is represented by the shaded area on the figure. Subsequent fragmentation may occur as the molecule relaxes along the excited state surface. The *threshold* energy for dissociation is the asymptotic limit of each potential curve at large A-B separation. With regard to the production of neutral fragments, a number of generalizations can be drawn from Figure 13: Firstly, it is obvious that the (Franck-Condon) transition energy to a dissociative state is significantly greater than the threshold energy. Secondly, the lowest threshold for neutral

dissociation is simply the A-B bond energy ... typically about 4 eV. Lastly, the threshold for dissociative ionization is the sum of the A-B bond energy and the ionization energy of A or B. Ionization energies are typically of the order of 10 eV. The threshold for dissociative ionization may be two to three times that for neutral dissociation. Similarly the Franck-Condon transition energy for dissociative ionization may be tens of eV greater than for neutral dissociation.

Dissociative attachment involves the essentially instantaneous excitation to an electronic state of the parent negative ion (AB^-) followed a relatively leisurely relaxation to fragments [47]. The relaxation, however, must compete with autodetachment of the electron. Dissociative attachment can only proceed if the electron-molecule complex persists for sufficiently long time for the parent negative ion to relax past a critical crossing point at R_c. The lifetime of the parent temporary negative ion is roughly inversely related to the energy of the attaching electron. Persistent negative ion states in some saturated molecules (alkanes, for example) typically involve the (resonant) capture of electrons with energies less than 1 eV. For unsaturated molecules (alkenes, alkynes) there may be long-lived negative ion states formed in the capture of electrons with energies up to 2 or 3 eV. Dissociative electron attachment has not been found to contribute to fragmentation in saturated hydrocarbons and fluorocarbons. Dissociative attachment is significant for many unsaturated hydrocarbons and unsaturated fluorocarbons as well as saturated chloro- and bromocarbons.

Electronic excitation to ground state of the parent ion deserves special attention in the present context. The ion, AB^+, having lost a strongly-bonding electron, tends to assume a geometry very different from the parent neutral as suggested by the displacement of the minimum of the ground state ion potential energy curve relative to that of the ground state neutral. Vertical excitation of the neutral to the bound state of the ion frequently leaves the ion with energy in excess of its dissociation limit. As a consequence, there are many chemical species for which the parent ion cannot be produced by electron impact.

The likelihood of any particular electron-impact-induced process is specified as a cross section [48]. In general, the cross section for electronic excitation as a function of the energy of the impacting electron rises from zero at the threshold to a broad maximum at the energy corresponding to the Franck-Condon region and then slowly decreases with increasing electron energy. The maximum cross section for the sum total of all electronic excitation leading to fragmentation (exclusive of dissociative attachment) typically reaches a maximum for an impacting electron energy of about 100 eV. The magnitude of the sum total cross section roughly amounts to the gas kinetic cross section of the target molecule, of the order of $10 \times 10^{-20}\,\mathrm{m}^2$. As suggested by the potential-energy diagram, the cross section for neutral dissociation peaks at lower energy (30-70 eV) than that for dissociative ionization (50-150 eV). Below 50 eV, neutral dissociation is usually the main source of radicals. Above 100 eV both neutral dissociation and dissociative ionization are important sources of radicals from electron-impact fragmentation of polyatomic molecules.

To determine the cross section for dissociation one must detect one or the other of the fragments. Experimentally it is much easier to detect a charged particle, so, if the choice exists, a charged fragment of dissociation is detected rather than a neutral fragment. This is obvious from the literature describing radical production by electron-impact; there are many more reports of measurements of cross sections for dissociative ionization than for neutral dissociation since a measurement of a neutral dissociation cross section requires the detection of one or the other of the neutral products.

Cross section measurements should be carried out under single-collision conditions. Real-time measurements of neutral dissociation cross sections require essentially single-radical sensitivity. Mass spectrometric and optical techniques are the obvious choices [49]. Optical methods can be very sensitive in the detection of atoms. For molecular species, however, transition intensity is spread over many rovibrational components of a transition, effectively reducing the sensitivity of optical detection of either emitter or absorber. In addition, optical techniques, such as laser-induced fluorescence, suffer a lack of generality; one must know in detail the spectrum of each species to be detected. On the other hand, a mass spectrometer can be employed to detect almost any volatile species at concentrations below $10^2\,\mathrm{cm}^{-3}$ owing to the fact that the typical electron-impact-ionization source ionizes all species with approximately the same high efficiency. This lack of specificity, however, may be a curse rather than a blessing. To measure a cross section for radical production, a beam of electrons is passed through a target gas at a sufficiently low density that only a small fraction of the target is dissociated; the radical precursor is present in much higher concentration than the radical. The problem that arises with mass spectrometric detection is that electron-impact ionization in the mass spectrometer source of both the radical products and the target gas yields the same ionic species. For example, the 69 amu CF_3^+ peak is the most

prominent feature in the mass spectrum of both the parent CF_4 and the radical fragment CF_3. As discussed above, the parent ion of the stable target molecule (i.e., CF_4^+) is not produced in the electron-impact source of a mass spectrometer. A degree of discrimination between parent and radical product has been achieved by adjusting the ionizer electron energy to the threshold for the species of interest (*vide infra*). Some specificity has also been achieved with a multi-photon ionization source.

Alkyl radicals react with many main group metals to produce volatile polyalkyl metal complexes. In 1929 Paneth and Hofeditz first demonstrated the existence of radicals in an experiment in which the photodecomposition products of an organic compound were exposed to a mirror of lead [50]. The disappearance of the mirror along with their detection and analysis for tetramethyl lead were essentially conclusive. Subsequently, Rice and Dooley [51] and Belchetz and Rideal [52] showed that methyl radicals reacted at a tellurium mirror to yield appreciable quantities of dimethyl ditelluride, dimethyl telluride, and a small quantity of hydrogen telluride.

Corrigan [53] and then Winters and Inokuti [54] took essentially the opposite tack in making the first quantitative measurements of the total dissociation cross section. Electron irradiation of a gas was carried out in a closed vessel whose walls were coated with a titanium getter that permanently sequestered radical fragments of electron impact dissociation. The total dissociation cross section was obtained from the pressure drop in the container, the irradiating beam current, and time of exposure. Employing these data, total neutral dissociation cross sections have been calculated for CH_4, CF_4, and C_2F_6 as the difference between the total dissociation and total ionization cross sections [55–61].

Motlagh and Moore developed a specific and nearly universal technique for the quantitative analysis of radicals that has been employed in the measurement of *partial* cross sections for the production of neutrals by electron impact on CH_4, CH_3F, CH_2F_2, CHF_3, CF_4, C_2F_6 and C_3F_8 [62]. (A partial cross section is a cross section for a process such as ionization or dissociation with the production of one specific product.) The technique, based on the method by which radicals in the gas phase were first identified, relies upon the efficient reaction of radicals with tellurium to yield volatile and stable organotellurides. A beam of electrons passes through a target gas in a collision cell that has a tellurium mirror on its inner surface. Radicals from electron-impact fragmentation react with tellurium within their first few encounters with the wall to produce volatile tellurides. (An electrical bias prevents ions from reaching the tellurium surface.) The telluride partial pressure is measured mass spectrometrically and related to the radical production rate. The technique is specific for radicals since a target gas of stable (even-electron) molecules does not react at the tellurium surface. In addition, the portion of the mass spectrum under observation is displaced by more than 128 amu (the nominal tellurium mass) from the region displaying peaks characteristic of the parent gas.

It can reasonably be argued that above the dissociation threshold the total dissociation cross section is equal to the sum of the cross sections for excitation to all available electronic and ionic states [54]. Following this line of reasoning, Mi and Bonham have carefully measured the total inelastic electron-scattering cross section (equivalent to the total excitation cross section) for N_2 and CF_4 and obtained the neutral dissociation cross section by subtracting the total ionization cross section [63].

Sugai and collaborators have worked to develop threshold-energy ionization/mass spectroscopy as a technique for observing radicals from electron-impact fragmentation (ref. [64] and references therein). The technique relies on the fact that the threshold for ionization of radical fragments is invariably 3 to 5 eV lower than that for the stable parent from which the radical is derived. To obtain radical specificity, the electron energy in the mass spectrometer ion source is set in the range below the ionization energy of the parent. Great care is required in setting the energy and controlling the energy width of electrons in the ion source since the concentration of radicals to be ionized and detected is typically orders of magnitude less than that of the parent. Sensitivity suffers; the ionization efficiency is low near threshold. This technique has permitted the determination of relative partial dissociation cross sections for the production of a range of neutral fragments for each parent that has been investigated. Placing the cross sections on an absolute scale has involved a difficult determination of a number of instrument variables and normalization to other measurements.

Perrin, Schmitt, De Rosny, Drevillon, Huc, and Lloret, derive dissociation cross sections from a kinetic analysis of molecular dissociation in a constant-flow multipole dc plasma reactor [65].

Including the measurements mentioned above, total dissociation or neutral dissociation cross

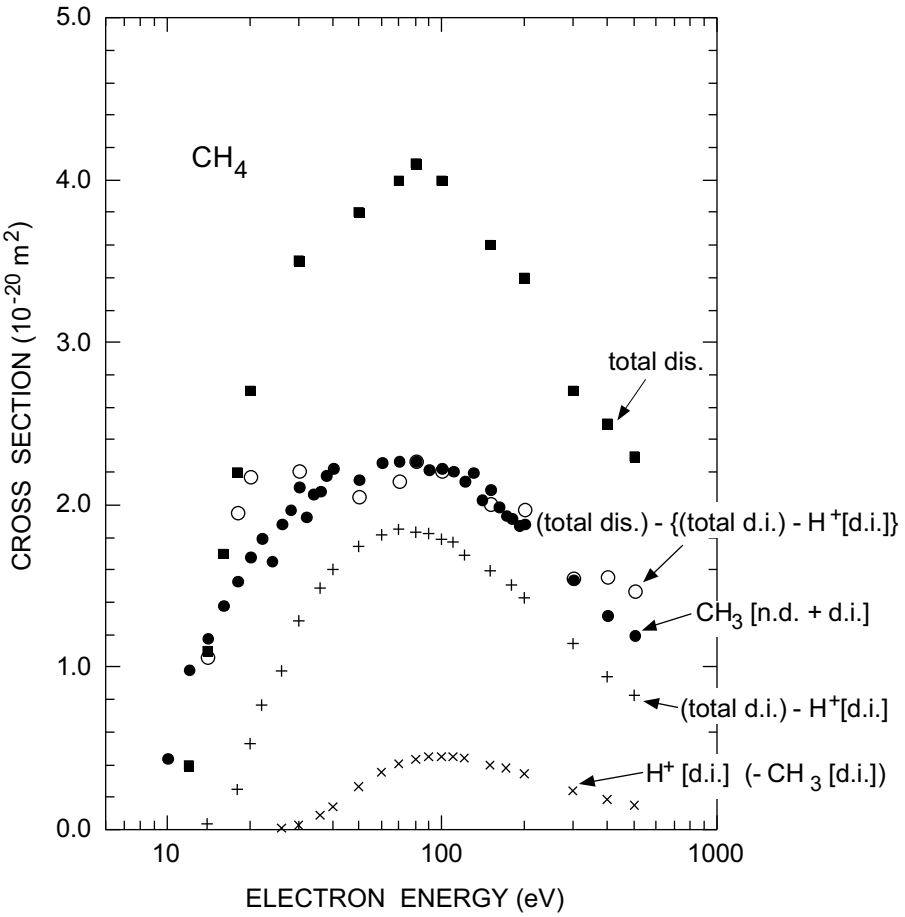

FIG. 14: Cross sections for the production of CH_3 resulting from electron impact on CH_4. The cross section for the production of CH_3 by both neutral dissociation and dissociative ionization [●, ('CH_3 [n.d. + d.i.]', Reference [62]] has been normalized to the difference (◯) between the total dissociation cross section (■, 'total dis.', Reference [65]) and the total dissociative ionization cross section apart from the contribution of dissociative ionization to CH_3 production (+, '(total d.i.) - H^+ [d.i.]', Reference [66]). The cross section for production of CH_3 by dissociative ionization is taken equal to the cross section for the production of H^+ by dissociative ionization (×, 'H^+ [d.i.] (= CH_3 [d.i.])').

sections have been reported for methane [67] (*vide infra*); all the fluorinated methanes [54, 62, 63, 68, 69]; perfluorinated ethane [54, 62], propane [62, 69] and cyclobutane [70]; C_3HF_7O [64]; silane [65] and disilane [65]. Several authors, notably Christophoru, Olthoff and Rao; [1, 71–73] Shirai and coworkers [74]; and Morgan [57], have undertaken reviews and evaluations of these data attempting to justify interrelated measurements such as total dissociation cross sections and cross sections for neutral dissociation and dissociative ionization, as well as partial cross sections for production of specific product fragments. Experimental data on electron-impact fragmentation of methane, CH_4, and perfluoromethane, CF_4, represent a significant proportion of what is available. By way of example we show a sample of data for the production of methyl radical (CH_3) from methane

(CH_4), and perfluoromethyl radical (CF_3) from perfluoromethane (CF_4). Neutral dissociation and dissociative ionization are the primary processes leading to electron-impact fragmentation for both CH_4 and CF_4; dissociative attachment is not significant in either case.

The two processes contributing to methyl radical production from methane are

$$e^- + CH_4 \rightarrow CH_3 + H + e^- \qquad \text{(neutral dissociation)} \tag{8}$$

$$e^- + CH_4 \rightarrow CH_3 + H^+ + 2e^- \qquad \text{(dissociative ionization)} \tag{9}$$

A collection of data bearing upon the production of CH_3 from electron impact on CH_4 is shown in Figure 14. The total dissociation cross section ('total dis.' in the figure) was obtained by Winters [65] using the gettering technique. The cross section for methyl radical production by reactions (8) and (9) (CH_3 [n.d. + d.i.]) was obtained with the telluride-conversion technique by Motlagh and Moore [62]. The cross section for reaction (9), the partial ionization cross section for the production of H^+, has been measured by Straub, Lin, Lindsay, Smith, and Stebbings [66], who also measured the total ionization cross sections ('total d.i.') as well as the partial ionization cross sections for the other the major dissociative ionization channels:

$$e^- + CH_4 \rightarrow CH_3^+ + H + 2e^- \tag{10}$$

$$e^- + CH_4 \rightarrow CH_2^+ + 2H \text{ (or } H_2) + 2e^- \tag{11}$$

$$e^- + CH_4 \rightarrow CH^+ + 3H \text{ (or } H_2 + H) + 2e^- \tag{12}$$

As implied by reaction (9) and indicated on the figure, the cross section for the production of H^+ by dissociative ionization is identical to that for the production of CH_3 by dissociative ionization ('H^+ [d.i.] (= CH_3 [d.i.])'). It follows that subtracting all the dissociative ionization, apart from this channel, from total dissociation leaves the cross section for CH_3 production. This subtraction is shown on the figure ('(total dis.) - (total d.i.) - H^+ [d.i.]'). The agreement with the direct measurement of total CH_3 production reflects the internal consistency of the various measurements.

With regard to generalizations about cross sections made in the introduction above, it should be noted that, for methyl radical production from electron-impact on methane, virtually all of the radical production is attributable to neutral dissociation below about 50 eV. The maximum cross section for radical production by neutral dissociation is at lower energy (∼70 eV) than for production by dissociative ionization (∼100 eV). The threshold energy for neutral dissociation (∼12 eV) is distinctly below that for dissociative ionization (∼18 eV).

A collection of data bearing upon the production of CF_3 from electron impact on CF_4 is shown in Figure 15. The two processes contributing to CF_3 production are

$$e^- + CF_4 \rightarrow CF_3 + F + e^- \qquad \text{(neutral dissociation)} \tag{13}$$

$$e^- + CF_4 \rightarrow CF_3 + F^+ + 2e^- \qquad \text{(dissociative ionization)} \tag{14}$$

Absolute neutral dissociation cross sections at three energies as reported by Mi and Bonham are shown on the figure [63]. These data represent the difference between their measurements of the total inelastic electron-scattering cross section and the total ionization cross section. Relative cross section measurements for CF_3 radical production by reactions (13) and (14) ('CF_3 [n.d. + d.i.]') were carried out employing the telluride-conversion technique by Motlagh and Moore [62]. These measurements are placed on an absolute scale by normalization to the Mi and Bonham cross sections under the assumption that neutral dissociation is the sole source of CF_3 radicals below about 40 eV. Cross sections for the production of F^+ have been measured by Ma, Bruce, and Bonham [75–77], and by Poll, Winkler, Margreiter, Grill, and Mark [78]. These data are in excellent agreement with one another. The recommended average [71] of these two sets of data (following various corrections [77, 79]) is shown in Figure 15. As implied by reaction (14) and indicated on the figure, the cross section for the production of F^+ by dissociative ionization is identical to that for the production of CF_3 by dissociative ionization ('F^+ [d.i.] (= CF_3 [d.i.])'). The cross section for the production of CF_3 by neutral dissociation ('CF_3 [n.d.]') is obtained as

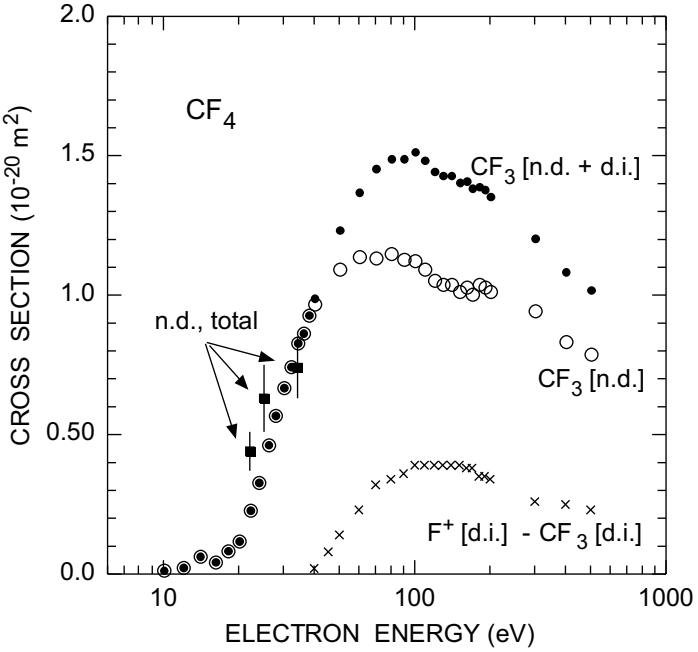

FIG. 15: Cross sections for the production of CF_3 resulting from electron impact on CF_4. The cross section for the production of CF_3 by both neutral dissociation and dissociative ionization (●, 'CF_3 [n.d. + d.i.]', Reference [62]) is normalized to the total neutral dissociation cross section (■, 'n.d., total', Reference [63]) below 40 eV where only neutral dissociation contributes. The cross section for production of CF_3 by dissociative ionization is taken as equal to the cross section for production of F^+ by dissociative ionization (×,'F^+ [d.i.] (= CF_3 [d.i.])', References [71, 75–79]). The cross section for the production of CF_3 by neutral dissociation (◯, 'CF_3[n.d.]') is taken as the difference between the normalized cross section for production of CF_3 by both neutral dissociation and dissociative ionization and the cross section for the production of CF_3 by dissociative ionization.

the difference between that for production by both neutral dissociation and dissociative ionization and that for dissociative ionization alone.

The data for electron-impact fragmentation of CF_4 support the generalizations above. For CF_3 radical production from electron-impact on CF_4, neutral dissociation accounts for virtually all of the radical production below about 50 eV. The maximum cross section for radical production by neutral dissociation is at lower energy (∼70 eV) than for production by dissociative ionization (∼120 eV). The threshold energy for neutral dissociation (∼18 eV) is distinctly below that for dissociative ionization (∼40 eV).

V. DISSOCIATIVE IONIZATION

A. Introduction

The processes which result in formation of the positive ions are known under the common name "Electron Impact ionization"- (EII). The description of the EII reactions is a complex task which includes many problems such as the kinetics, energetics of the reactions, the mechanism of ion formation, the dissociation and the distribution of products. Several reviews and books have been

written on this topic over the years. We note in particular the review by Märk [80], Märk and Dunn [81] as well McDaniel [82], Illeneberger and Momigny [83], Christophorou and Olthoff [1] and reviews by Becker and Tarnovsky [84].

According to [7] the dissociative ionization (DI) is the most relevant EII reaction channel to the FEBIP technique. We will try to present some essential aspects of EII and DI processes which may be interesting for the FEBIP user. The dissociative ionization depends on the size of the molecule, its chemical composition, structure, initial state and the energy of the interacting electrons. In the case of organometallic molecules we deal with large polyatomic molecules and the number of the dissociative channels may be very large. For the FEBIP technique, those DI channels are important, which lead to formation of small fragments (ionic or neutral) with metal atom inside. In ideal case "naked" metallic ions or "naked" metal atoms are formed which can be deposited on the surface and form metallic layers. Detailed knowledge of the dissociation processes and their cross-sections at electron energies relevant for FEBIP technique would enable to select suitable precursor molecules and tune the electron energy, and thus finally improve the performance of this technique. Unfortunately, so far only very little was done on the field DI to organometallic compounds, especially concerning the kinetics of these reactions.

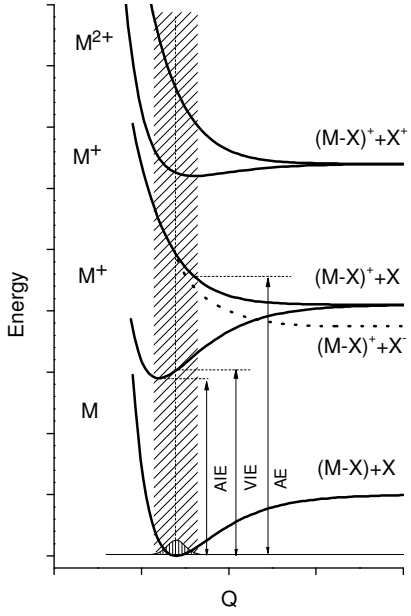

FIG. 16: Potential energy curves of molecule M and the different ionic states M^+, M^{2+}, fragment ions $(M\text{-}X)^+$, X^+, X^-, and the neutral fragment, or radical, X. Q is one of the molecular reaction coordinates. AIE – adiabatic ionization energy, VIE – vertical ionization energy, AE – appearance energy of the ion $(M\text{-}X)^+$.

B. Electron-impact ionization

The EII generally, is the interaction of the electrons with a neutral targets (molecules or atoms), which results in formation of a positively charged particles (molecular ions, fragment ions, metastable ions, multiply charged ions ...), two or more electrons and also neutral fragments or radicals. In the case of EII to the atomic and molecular targets single and multiple ionizations are possible reaction pathways:

$$
\begin{aligned}
e^- + M &\rightarrow M^+ + e_s^- + e_e^- && \text{single ionization} && (15)\\
&\rightarrow M^{n+} + e_s^- + n e_e^- && \text{multiple ionization} && (16)\\
&\rightarrow M\text{-}R^+ + R^+ && \text{Coulomb explosion} && (17)\\
&\rightarrow M^{(K)+} + e_s^- + n e_e^- && \text{innershell ionization} && (18)\\
&\rightarrow M^{**} \rightarrow M^{*+} + 2e^- && \text{auto-ionization} && (19)\\
&\rightarrow M^{*+} \rightarrow (M\text{-}R)^+ + R && && (20)
\end{aligned}
$$

In addition, in the case of molecular targets (as it is in case of organometallic molecules), dissociative channels – dissociative ionization (DI) occurs:

$$
\begin{aligned}
e^- + M \rightarrow M^{*+} &\rightarrow (M\text{-}R)^+ + R + e_s^- + e_e^- && \text{dissociative ionization} && (21)\\
&\rightarrow (M\text{-}R)^+ + R^- + e_e^- && \text{ion pair formation} && (22)
\end{aligned}
$$

M - denotes the neutral target, R – the neutral fragment or radical, M^+ – ions, e_s^-, e_e^- – "scattered" and "ejected" electrons. The reaction (22), called "ion pair formation", is often reported along with dissociative ionization, however, in contrast to the dissociative ionization the fragment R is negatively charged. The process of dissociation may be fast if it occurs on the timescale of pico-seconds or metastable if the life time of the unstable ion spans from nanoseconds up to microsecond scale.

High energy electrons have the ability to induce multiple ionizations (16). The stability of the multiply charged ions depends on the electronic structure and geometry of the molecular ions and on the elemental composition of the multiply charged ions. The multiply charged ions may further decompose *via* a process called Coulomb explosion (17). This process occurs if the repulsive Coulomb force of the two (or more positive charges) in the multiply charge ion exceeds the intramolecular forces which bind the molecule together.

The electron impact ionization is a fast process for which the Born-Openheimer approximation is valid (Figure 16). Typical time scale for direct ionization event is 10^{-16} s, which is much shorter then a typical vibrational period of a molecule. This means that during the ionization event we neglect the movement of the molecular nuclei. This fast process we call direct ionization. By varying the incident electron energy we are able to reach different bound states of the molecular ion and also the states of the continuum.

Positive ions may be formed also *via* an indirect mechanism, e.g., auto-ionization (19 and 20), where the molecules are excited to doubly excited states, which decay radiationlessly into an ion M^{*+}, which may further dissociate. The indirect processes can be recognized by the structures in the measured ionization cross sections as the process has resonant character. In some atoms and molecules the indirect ionization may play important role [81, 84].

The EII and DI are generally endothermic reactions, i.e., there exists for each of the reactions a particular threshold and only electrons with an kinetic energy above this threshold may initiate the reaction. In the case of the reaction EII the threshold is called ionization energy (IE) of the particle (atom or molecule). Typical values of the ionization energies of the molecules are in the range of 10 eV [85]. The values of the ionization energies reflect the chemical composition, the electronic structure of the molecule, the geometry and the internal energy of the molecules prior to the reaction.

If the incident energy of the electron exceeds the dissociation limit of the molecular ion state (Figure 16), dissociative ionization may occur (reaction channel (21)). The dissociative ionization proceeds *via* the formation of the excited molecular ion M^{*+} which decays further into fragment ions - primary ions and neutral fragments. The primary ions with excess of energy may further decompose into secondary ions. The molecules fragment into i) ions which contain functional group, ii) ions formed by cleavage of a functional group and iii) ions formed *via* rearrangement of the bonds within the ion [86]. The fragmentation of the molecule can be theoretically treated quantitatively only for small molecules (diatomic and small polyatomic). The potential-energy surfaces of the neutral and ionic states can be calculated using *ab initio* quantum chemical methods and the dissociation can be treated in terms of molecular dynamics. For larger polyatomic systems (inclusive majority of the organometallic molecules) the quasiequilibrium theory provides a tool to

study the dissociation of the ions [86]. Lango *et al.* [87] applied quasi-equilibrium theory to study unimolecular decay of the organometallic ions.

The cross section is generally a quantity which describes the probability of the ionization of electrons with given kinetic energy interacting with molecules; it has the dimension of an area (usually the units are m^2, cm^2). The total ionization cross section gives the probability of the formation of any positive ion without detailed information about the nature of the ions formed. The partial ionization cross section reflects the efficiency of formation of a specific ion (molecular ion, fragment ions, multiply charged ion).

The theory of the ionization reaction is a complex task, because the ionization is a many body problem, which is not trivial to solve rigorously. Therefore mainly semiempirical methods are employed to calculate total cross sections for EII. There exist several semiempirical methods based on the additive rule [88], which express the total single ionization cross section as the sum of the ionization cross sections of the constituent atoms. These methods have limitations, since molecular bonding is not taken into account. Therefore new concepts (modified additive rule) have been proposed which attempt to account for the molecular bonding [89], and which give reasonable agreement in total ionization cross section for whole range of molecules. A different semiempirical method is the so called DM formalism introduced by Deutsch and Märk [90]. In recent years the Binary Encounter Bethe (BEB) of Kim [91] gained recognition with very good results for atmospheric and hydrocarbon molecules. The usability of this method should be proofed for organometallic compounds.

The situation on the partial cross sections for DI is even more complicated. Generally the most reliable information about total DI cross section can be obtained at present time using experimental methods. The overview of various experimental methods employed to study EII and DI can be found in [80, 81, 84]. Dissociative ionization has been intensively studied experimentally already for several decades. Dedicated experimental techniques were developed to study EII [81, 82], which allow to measure absolute or relative double and triple differential ionization cross sections.

Absolute partial and absolute total ionization cross sections, on the other hand, are the result of experiments which are not differential in electron scattering angle, energy of the outgoing electrons and electron spin. For many areas of applications (plasma physics, electric discharges and also FEBIP) angle-integrated absolute total cross sections and absolute partial cross sections (mass selected) are of high importance, as these cross sections govern the production rate of a variety of reactive species and secondary electrons. In recent decades advance in measurement of absolute DI cross sections has been achieved, however, some problems still persist: i) achievement of reliable detection efficiency of the mass spectrometers for ions with different masses; ii) discrimination effects at the ion source; iii) in the case of the dissociative ionization, problems with kinetic energy release. For a detailed discussion of the advantages and limitations of the various experimental setups see [82]. At present time several laboratories in the world master the technique of measurement of absolute partial cross sections for DI, e.g., see the following articles [92–96].

Besides the cross section, the experiment may provide also other quantities like ionization energies of the molecules and the appearance energies of the fragment ion formed upon DI. From these quantities we may obtain information about the structure of the molecule, of the molecular and fragment ions and the reaction enthalpies of the dissociation channels.

C. Dissociative ionization of molecules

The number of molecules for which absolute ionization cross sections are available increases only slowly. Most of the molecules are simple di-atomics H_2, N_2, O_2, CO, NO, and HCl, and tri-atomic molecules such as H_2O, CO_2, N_2O, NO_2 and SO_2 [84]. The studies of polyatomic molecules were stimulated largely by the need for ionization cross section data in various areas of applications (C_2H_2, NH_3, CH_4, CCl_4, CF_4, SF_6, Si_2H_6, C_2H_6 and C_3H_8 (see [81, 84] for a more complete list of references). In the past decade the list grew only very slowly. For molecules the single ionization processes are the dominant mechanisms, whereas multiple ionization and ion pair formation tend to have much smaller cross sections.

The importance of DI increases with the size of the molecules. In many molecules the cross sections for the formation of fragment ions are larger than the parent ionization cross section (C_2H_6, CF_4, NF_3 ...) [84]. The initial state of the molecules has also an influence in the DI processes [104, 105], it may influence (decrease) the appearance energy of the fragment ions and

TABLE I: The ionization energies (IE) of selected organometallic molecules, the appearance energies (AE) of the metal atom ions Me^+, and the relative abundances of Me^+ in mass spectra at electron energy of 70 eV (ratio (Me^+/Total ion intensity)).

Molecule	IE (eV)	AE(Me^+) (eV)	Method	Relative Me^+ intensity
$Al(CH_3)_3$	9.09 ± 0.26	14.6 ± 0.2	EI [97]	16% [98]
$Ga(CH_3)_3$	9.87 ± 0.02	13.24 ± 0.03	EI [99]	27% [98]
$Co(CO)_3NO$	7.89 ± 0.3	14.03 ± 0.3	EI [100]	21% [100]
$CpCo(CO)_2$	7.08 ± 0.3	13.47 ± 0.3	EI [100]	11% [100]
Cp_2Co	5.35 ± 0.3	14.19 ± 0.3	EI [100]	12% [100]
$(RhCl(CO)_2)_2$	9.01	–	PE [101]	10% [85]
$Re_2(CO)_{10}$	8.49 ± 0.02	28.96	PE [102]	<1% [85]
$(CH_3C_5H_4)_2Fe$	6.6 ± 0.2	14.9 ± 0.3	EI [103]	1.5%[103]

also change the distribution of the fragments.

The needs for the cross sections and other data concerning EII and DI to organometallic molecules relevant to FEBIP applications are very large. The kinetic data are of high importance for understanding processes involved in these techniques, for computer modeling and optimization of the processes. For majority of the organometallic compounds the cross sections for EII and DI were not measured so far. In fact, we have found only few publications with partial cross sections for DI of organometallic molecules. Jaio *et al.* [98] measured total ionization cross section to trimethyl-aluminum (TMA) and trimethyl-gallium (TMG) molecules. They applied Fourier Transform mass spectrometry with electron ionization source to measure partial cross sections for DI to TMA and TMG molecules. The Figure 17a presents the measured cross sections for TMA, TMG in Figure 17b shows very similar cross sections and fragmentation pattern. The dominant product in the whole measured energy range was the $Al(CH_3)_2^+$ ion. The parent molecular ion was more then one order of magnitude weaker. This indicates that the molecular ion decays rapidly into other products. A very interesting result of this study is the fact that the metal ion Al^+ is the second most abundant species formed at electron energies above 20 eV (see Table I). In the case of TMG (Figure 3.1b) there is a very similar picture with one important difference that the cross section for metal ion Ga^+ has the second largest cross section in the whole measured energy scale. The Ga^+ ions makes, at 70 eV, almost 27% of all the ions formed.

A more reliable method of partial cross section measurements was applied by Popovic [106], who

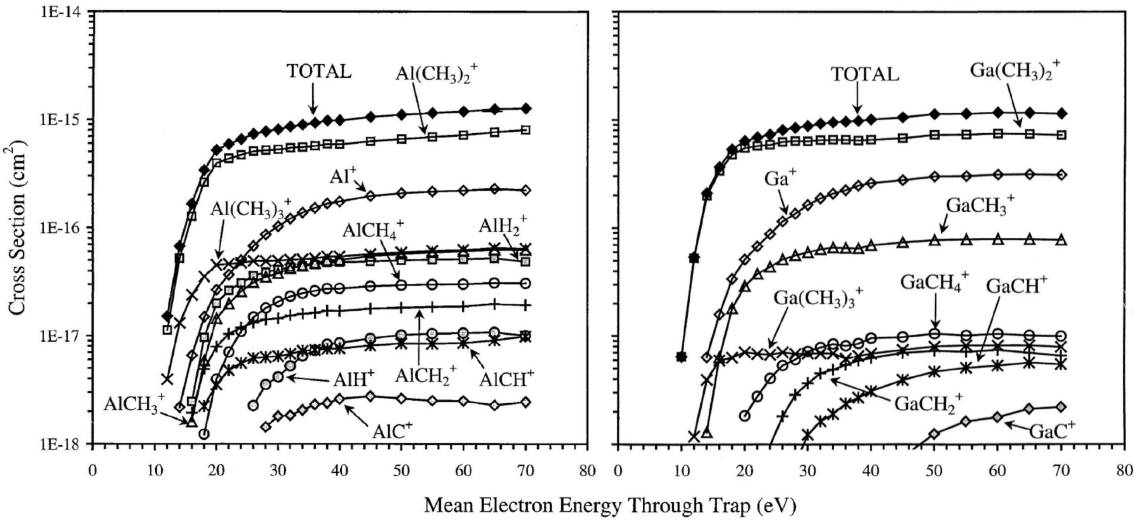

FIG. 17: Partial cross sections for dissociative ionization of a) TMA b) TMG. Reprinted from [98] with permission from Elsevier.

measured partial cross sections for DI to Barium derivatives (BaO, Ba, BaF_2 and BaI_2). Basner *et al.* [107] investigated EII to CpPtMe$_3$ - $(C_5H_5)Pt(CH_3)_3$, $(MeCp)_2Ru$ - $(CH_3C_5H_4)_2Ru$ and $(MeCp)_2Fe$ - $(CH_3C_5H_4)_2Fe$. They measured ionization energies, total ionization cross sections and also mass spectra of the molecules. The contribution of metal atom ions was according to this work small.

Another type of DI experiments is the study of the threshold behaviour of the mass selected ion yields. Opitz [100] in his study to several organometallic compounds of cobalt measured the mass spectra of the molecules and in addition also ionization energies of the molecules and appearance energies of the fragment ions. From the appearance energies he determined some important quantities, like bond dissociation energies of various functional groups in the molecules and heats of formation of molecular ions and selected fragment ions. Similar studies were done also for molybdenum complexes [108], ferocene and chloro-ferocene [109].

For many organometallic compounds electron ionization mass spectra are available, ionized typically by 70 eV electrons ([110–113] ...) Electron ionization mass spectroscopy is with NMR and IR spectroscopy a standard tool which is used to characterize synthesized molecules. The mass spectrometric studies give some basic information about the structure of the molecules, the functional groups of the molecule, about fragment ions formed by DI. These data do not provide information about the cross sections as a function of electron energy and about the thresholds of the DI channels.

Information about the ionization energies, threshold energies for DI processes can be obtained from other types of experiments, (photo ionization [114], or photoelectron spectrometry [101, 115, 116]) and quantum chemical calculations [117, 118]. Except of electron ionization mass spectrometry, several different ionization methods were applied to study mass spectra of the organometallic molecules (field ionization [119], VUV photoionization [114, 120], multi-photon ionization [121]).

The molecular targets relevant to FEBIP technique are various organometallic compounds which decompose under electron impact into fragments (neutral and ionic), which contain a metal atom and dissociate at some extent into metal atoms and metal atom ions. These particles then may deposit on the surface and form metallic structures. The products of DI reaction may also undergo ion-molecular reactions [122] and chemical reactions on the surface, which may modify the composition of the metallic structures.

The dissociative ionization of the organometallic molecules may be initiated by the primary electrons (with kinetic energies in the range of several tens of keV). However, we should not underestimate also the role of the secondary electrons to initiate DI reaction in FEBIP. The relative contribution of secondary electrons to DI events may in some systems comparable with the contribution of primary electrons. There exist several reasons for this implication: i) the cross sections for DI and EII generally decrease with the increasing electron energy and thus for primary electrons (kinetic energy in the range of tens of keV) the cross sections for DI could be relatively small, ii) the ionization energies of the organometallic compounds and the DI thresholds are usually low (often far below 10 eV see Table I) even for metal atom ions, thus iii) the thresholds for DI are within the interval energies of the secondary electrons.

VI. ELECTRON-INDUCED REACTIONS IN THE CONDENSED PHASE

The previous sections have shown that electron-molecule interactions in gas-phase induce chemical reactions, namely, dissociative electron attachment (DEA), dissociative ionization (DI), and neutral dissociation (ND). The same processes can also be induced in condensed phases or adsorbates on surfaces, the latter being the situation relevant to FEBIP. The dense environment in such systems, however, can modify the outcome of the initial electron-molecule interaction. Furthermore, it offers reaction partners to the initially formed reactive fragments. Consecutive reactions thus occur and have to be considered to understand the final products of electron-induced chemistry. Also, while gas-phase studies are capable of detecting the immediate reactive products of the initial electron-molecule collision, the consecutive reactions in the condensed phase may occur so rapidly that only stable, i.e., closed-shell, final products can in fact be monitored. Typically, because the chemistry of highly reactive fragments often is not very selective, electron-induced reactions in the condensed phase yield a complex mixture of products which can, as an additional complication, usually not all be detected by the same method. Different analytical techniques are

therefore, in the ideal case, applied to the same system. An experimental procedure that separates different products after the electron exposure is useful but may by itself induce more consecutive reactions.

The meaning of cross sections derived from condensed-phase measurements requires specific attention. For example, a cross section for formation of a specific product may refer to a sequence of elementary reaction steps in which the electron-molecule interaction is only the initiating process. Equally, if the detection of a product requires its thermal desorption from a surface or a condensed phase, the thermal activation may lead to additional reactions so that the detected product is not necessarily the one that was initially formed by electron-induced chemistry. This section discusses selected examples of electron-induced reactions in a condensed phase. Typical methods applied to condensed-phase electron-induced reactions are presented first. The effect of the condensed phase on the initial electron-molecule interactions is then addressed and examples are presented that underline the importance of intermolecular reactions. Finally, examples of cross-section measurements are discussed.

A. Methods for studying electron-induced reactions in condensed phases

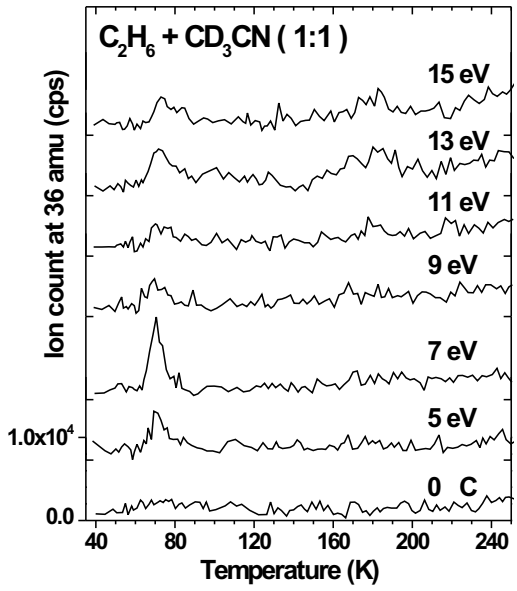

FIG. 18: TDS recorded at 36 amu of a multilayer mixture of ethane (C_2H_6) and deuterated acetonitrile (CD_3CN) before and after electron exposure of 1800 $\mu C/cm^2$. The desorption peak between 70 and 75 K is ascribed to formation of C_2D_6 [123].

Due to the restricted penetration depth of electron beams [124] surface science methods are applied to the study of electron-induced reactions, the most frequently used being electron-stimulated desorption (ESD), both of ions [125, 126] and neutrals [127, 128], thermal desorption spectrometry (TDS) [123, 129], X-ray photoelectron spectroscopy (XPS) [128, 130], high-resolution electron energy loss spectroscopy (HREELS) [131, 132], reflection-absorption infrared spectroscopy (RAIRS) [128, 130, 133], and low-energy electron transmission (LEET) [134]. In these experiments the samples must be conductive to avoid excessive charging during exposure to the electron beam. This calls for thin multilayer films or monolayer adsorbates on conductive surfaces. In contrast to the actual FEBIP process, the experiments are performed under ultrahigh vacuum (UHV) to avoid

adsorption of unknown amounts of residual gas and thus be able to control the composition of the sample. UHV requires that the experiments are performed at low temperatures to obtain a sufficient and well defined surface coverage. On the other hand, small product molecules can be trapped at low temperature and thus identified following electron exposure. Nonetheless, experiments in which a room temperature surface is exposed to a stream of the FEBIP precursor molecules during electron exposure and which thus simulate the actual FEBID process are possible [135]. Also, the clean environment can be exploited to study the effect of impurities like the residual gases present in FEBIP by admixing them in a controlled manner.

Motivated by the wish to understand the effect on the radiation chemistry of low-energy secondary electron that are formed abundantly under exposure to high-energy beams, many experiments so far have focused on electrons with kinetic energies below 20 eV. Nonetheless, commercial electron guns that are frequently used in these experiments can be tuned to energies up to 500 eV. Typical current densities applied to the samples are of the order of a few μA/cm^2. To achieve sufficient sensitivity, sample areas of 1 cm^2 and more are used.

As mentioned in the outline, different methods used in the study of electron-induced reactions of adsorbates and condensed phases have specific advantages and disadvantages. For example, the frequently used XPS yields information on elemental composition of the sample and the oxidation state of the elements but care must be taken to avoid extended X-ray exposure as secondary electrons themselves are known to induce reactions [136]. ESD mass-spectrometrically detects fragments desorbing under electron exposure but has little sensitivity towards heavier species which often do not have sufficient kinetic energy to overcome the barrier at the interface between molecular film and the vacuum which results from attractive forces within the condensed phase. LEET is complementary in the sense that it can be used to measure the charging of the sample which can be traced back to electrons or ions trapped within the sample. Methods measuring vibrational excitation spectra (HREELS, RAIRS) provide information on species remaining in the film. HREELS, on the other hand, can be difficult to interpret when a mixture of products is formed and their bands overlap. RAIRS has a better resolution but suffers from lower sensitivity. Finally, different products can be separated from each other because of their different desorption temperatures by using TDS which monitors the neutral species desorbing upon temperature increase of the sample.

Despite the fact that one can not easily distinguish if products detected by TDS have been formed as an immediate consequence of electron exposure or only after activation due to the temperature increase, this method has recently provided valuable insight into the mechanisms of electron-induced reactions by comparing with TDS experiments on samples with known composition [137]. Based on this it is possible to reliably identify products [138, 139] and also to determine cross sections for the formation of specific products [139]. The discussion of condensed-phase electron-induced reactions will specifically focus on some of these results but other important literature will be included as well.

The examples that will be discussed here to demonstrate the level of insight that can be obtained into condensed-phase electron-induced reactions concern simple organic compounds such as may be used for depositing carbonaceous deposits in FEBIP as well as hexamethyldisiloxane (HMDSO), a silicon-containing precursor. Nonetheless, a few UHV studies using the methods described above have been performed on the metalorganic FEBIP precursors $W(CO)_6$ [140], ferrocene ($Fe(C_5H_5)_2$) [141], $Mo(CO)_6$ [142], and trimethyl(methylcyclopentadienyl)platinum(IV) ($MeCpPtMe_3$) [128, 135]. The most comprehensive study so far concerns the latter compound and includes a comparison of cross sections for its decomposition obtained from XPS, RAIRS, and ESD [128].

B. Effect of the condensed phase or surface on intermediates and reactive products of electron-molecule interactions

By embedding a molecule in a condensed phase, the formation and evolution of neutral or ionic excited species produced by electron-molecule interaction is modified with respect to the gas phase. These effects have been summarized recently [143–145] and need not be repeated in detail although a few effects may be highlighted here.

In general, a condensed phase is a polarizable molecular environment which energetically stabilizes charged states or states with higher dipole moment with respect to the gas phase or to a neutral or less polar ground state. Charged states in a condensed phase are thus typically formed at slightly lower electron energy than in the gas phase. This modifies the relative energies of the

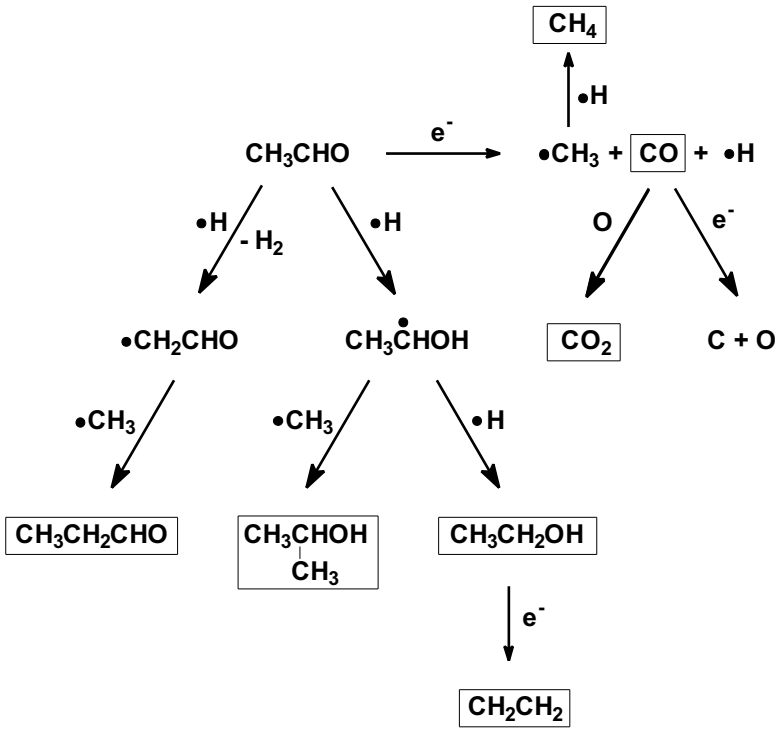

FIG. 19: Products identified in TDS measurements of multilayer films of acetaldehyde (CH_3CHO) after electron exposure at 15 eV [139]. Boxes mark the products that have been identified by TDS.

various electronic potential energy curves and can, for example, change the position of the critical crossing point and thus the branching ratio between autodetachment and fragmentation. Also, a negative ion state may drop in energy below a neutral state that would, in the gas phase, be the product of autodetachment thereby increasing the lifetime of the charged state and enhancing its fragmentation probability. Similarly, by energy transfer to neighbouring molecules, a negative ion state with potential energy minimum below the neutral ground state and thus accessible to free electrons only via its vibrationally excited states may undergo vibrational relaxation and thus form a stable negative ion. This contributes to charging of a condensed phase under electron exposure. Distance-dependent charge transfer to an adjacent metal surface can deactivate negative ion states and thus suppress fragmentation. Furthermore, thermalisation of the incoming electrons through multiple scattering in the condensed phase needs to be considered as it lowers the average energy at which an individual electron-molecule interaction takes place. As a final example, dissociation processes can be hindered in a condensed phase by the so-called cage effect which prevents the fragments from drifting apart and thus favors recombination.

The question relevant to FEBIP is if gas phase data on electron-induced fragmentation processes are in fact useful for understanding the corresponding condensed-phase chemistry. While DEA, DI, and ND are equally possible in the condensed phase, although at more or less modified electron energy, the fragmentation cross section can be modified by orders of magnitude [144, 145]. Because of a delicate balance between the different effects listed above, the actual deviation from the gas phase behavior needs to be considered separately for each specific case. Furthermore, the fragments resulting from electron-molecule interaction may simply recombine with other fragments or may decay themselves if the excess energy gained by formation of the new bond is sufficient to dissociate other bonds.

An example where a known gas-phase resonance survives in the condensed phase and leads to the expected product is shown inFig. 18. In the gas phase, DEA to acetonitrile (CH_3CN) in the energy range between 6 and 8 eV leads to dissociation along the CC bond as detected by formation of a dominant negative ion CN^- and smaller quantities of CH_3^- [146]. In the condensed phase, formation of C_2D_6 from deuterated acetonitrile is observed predominantly at 7 eV [123]. The

same DEA process is thus active in the condensed phase and the resulting neutral CD_3 fragments recombine to yield the stable product C_2D_6. In contrast, recent results on ammonia (NH_3) in the condensed phase [147] have shown that a DEA process in the 7-11 eV range detected as ESD of D^- from ND_3 [125] and consequently leaving behind ND_2 radicals does not yield N_2D_4. In contrast, production of N2 is observed. This suggests that ammonia is particularly easy to decompose to volatile fragments by electron exposure and is thus probably a suitable ligand for FEBIP precursors.

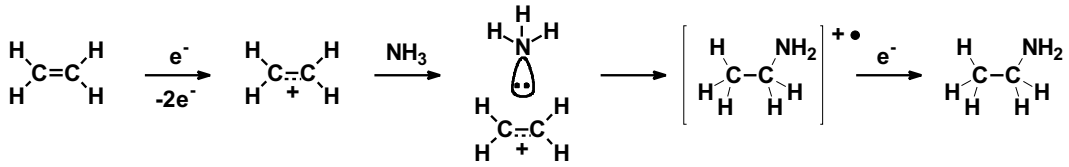

FIG. 20: Synthesis of aminoethane ($CH_3CH_2NH_2$) in multilayer mixed films of ethylene (C_2H_4) and ammonia (NH_3) induced by electron impact ionisation [148].

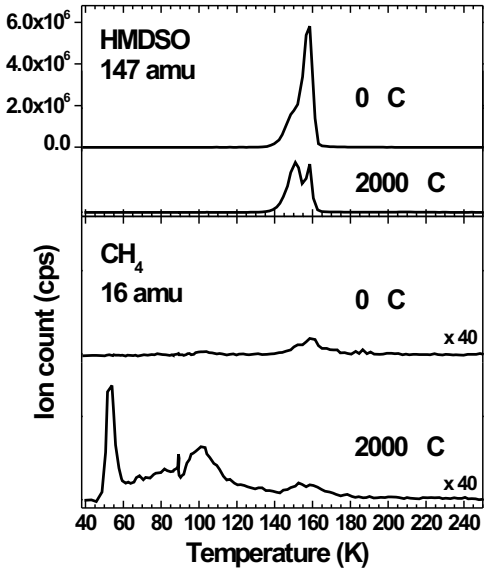

FIG. 21: TDS showing the depletion of hexamethyldisiloxane (HMDSO, 147 amu) from a multilayer films and the formation of methane (CH_4, 16 amu) in the same film upon electron exposure at 15 eV [149]. The integrated desorption signal for CH_4 serves as measure of the produced amount in the determination of the formation cross section.

C. Molecular synthesis induced by electron-molecule interactions

In FEBIP the desired outcome of the electron-molecule interaction is complete fragmentation to the point where only the desired element remains on the surface and all other fragments have sufficient volatility to desorb. While the previous sections on electron-molecule interactions in the gas phase have also emphasized fragmentation, in the condensed phase these initiating reactions are very likely succeeded by formation of new bonds driven by the reactivity of fragments with unpaired electrons [156]. These reactions can lead to the synthesis of stable larger and thus less volatile species and, in the extreme case, large-area crosslinking of the irradiated material [130]. Such reactions may well be responsible for the often remaining impurities in the deposits formed

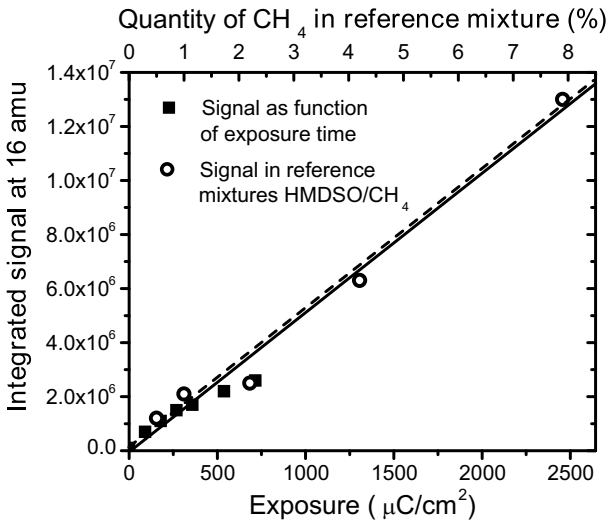

FIG. 22: Plot of the integrated desorption signal recorded at 16 amu (CH_4) as function of electron exposure at 15 eV and plot of the same integrated intensity for reference mixtures as function of CH_4 content [149]. The data yield a cross section of 5.1×10^{-18} cm^2 for the formation of CH_4.

under FEBIP. Therefore, a few examples shall illustrate the mechanisms of reactions taking place in electron-induced synthesis.

The first example concerns the reactions of acetaldehyde (CH_3CHO) [139], a molecule that releases important amounts of CO under exposure to electrons above roughly 10 eV. To form this product, two bonds must dissociate, initially yielding H and CH_3 radicals. It has been shown by use of TDS that these highly reactive species not only recombine to form CH_4 but can also react with neighboring intact molecules as summarized inFig. 19. These reactions synthesize a variety of products, some of which in fact larger than the parent compound acetaldehyde. It must be noted that in addition to the radical mechanisms shown inFig. 19, recent unpublished quantum chemical calculations provide evidence that some of the products and more specifically 2-propanol ($(CH_3)_2CHOH$) may be formed via cation-driven chemistry.

Another example shows convincingly that ionization-driven chemistry can contribute to the formation of larger and more complex species [148].Fig. 20 shows that ionization of ethylene (C_2H_4) initiates the synthesis of a larger product because the cation interacts attractively with a neutral molecule, in this case ammonia (NH_3), that carries a partial negative charge. Above the ionization threshold ethylene and ammonia thus react to form aminoethane ($CH_3CH_2NH_2$) as again deduced from TDS results. Alternatively, an equivalent reaction mechanism starting with ionization of ammonia can be conceived [148].

Other examples of the synthesis of larger species under low-energy electron exposure include the formation of deuterium peroxide (D_2O_2) from deuterated water (D_2O) [150], the production of ethylene glycol ($HOCH_2CH_2OH$), ethanol (CH_3CH_2OH), dimethyl ether (CH_3OCH_3) in methanol (CH_3OH) multilayers [129], the synthesis of the amino acid glycine (H_2NCH_2COOH) from mixtures of ammonia (NH_3) and acetic acid (CH_3COOH) [151], as well as the formation of various larger fluoroiodocarbons from trifluoroiodomethane (CF_3I) [152] and of different chlorocarbons from carbon tetrachloride (CCl_4) [153].

D. Cross sections for electron-induced reactions in condensed phases

Based on the described UHV surface analytical methods, cross sections for electron-induced reactions in the condensed phase can be obtained. Due to the specific interest in DEA, these measurements were so far often restricted to the 0-20 eV range [131, 139, 144], although experiments aiming at FEBIP precursors presently extend this range to energies reaching up to 1 keV [128].

Reference [144] summarizes different approaches to cross section measurements including XPS experiments aiming at cross sections for specific surface modifications, HREELS studies measuring the production of CO from an oxygen-containing organic compound, cross sections for dissociation and desorption of molecules from a surface obtained by mass spectrometry, and LEET experiments from which cross sections for charge trapping, both as solvated electron or in the form of stable anions or anionic fragments resulting from DEA can be deduced.

The measurement of cross sections for the decay of the initial sample is a relatively simple task because, under the condition of constant electron current density on the surface and assuming that reactions are initiated by a single electron-molecule collision, it follows simple first order kinetics [123, 128]. In contrast, it is more difficult to deduce values for the various products of electron-induced reactions. This is due to the fact that not all methods, especially those giving information on the chemical identity of a molecular product (RAIRS, HREELS, TDS), yield an absolute measure of the quantity of material. In such cases, signals must first be chosen that can unequivocally be ascribed to a specific product such as the lowest electronic excitation which is used for the quantification of CO in HREELS [132, 139, 144] or a specific desorption signal with a characteristic molecular mass and desorption temperature in TDS [139, 149, 154, 155]. Then the absolute intensity of these signals must be determined by comparing with reference samples containing a known amount of the product. An example of such a procedure using TDS is shown in Figs. 21 and 22. Here, the production of CH_4 from hexamethyldisiloxane (HMDSO) is quantified from its characteristic desorption signal recorded by setting the mass spectrometer to 16 amu. Fig. 21 also includes the desorption signal for the parent compound HMDSO recorded at 147 amu. The desorption of CH_4 starts with a sharp peak at 55 K but also extends up to the desorption temperature of HMDSO (140-165 K) because a part of the product quantity is trapped in the condensed HMDSO film. This is proven by reference samples which show a similar behavior [149]. Integration of the CH_4 desorption signal over the complete temperature range up to 165 K thus yields a measure from which the produced amount of CH_4 can be quantified by comparison with the same value obtained from the reference samples as shown inFig. 22. From this plot, the cross section for formation of the product can easily be calculated taking into account the number of electrons applied to the film and the surface area. This is explained in detail in [154].

A comprehensive UHV study on cross sections for degradation under electron exposure has been dedicated to the FEBIP precursor $MeCpPtMe_3$ [128]. This example shows that different methods must be applied to both follow the deposition of the desired element (XPS) and the decomposition of the organic material (RAIRS, MS). An increasing use of TDS in the future is anticipated to yield more detailed information on the chemical nature of the organic material remaining on the surface. The method described above may thus be of interest for fundamental studies on the chemical processes related to FEBIP.

VII. CONCLUSIONS AND OUTLOOK

Complete sets of cross sections, covering all the above processes and the entire energy range, are very rare. The choice of the targets for the measurements in the past was influenced by potential applications in plasma processing for semiconductor manufacture. An example are the cross sections for CF_4 and SF_6 given in the book of Christophorou and Olthoff, ref. [1], on pages 6 and 727, resp. In view of the emerging FEBIP application it would be desirable to measure similar cross section sets at least for several prototype FEBIP precursor molecules. Such an enterprise promises to be interesting also from the purely scientific point of view–by directing the attention of the electron-collision community toward metalorganic compounds.

Dissociative ionization may be the process most relevant to FEBIP. It may be initiated by both the primary electrons (with kinetic energies in the range of several tens of keV) and the secondary electrons. The relative contribution of secondary electrons may in some systems comparable with the contribution of primary electrons because the cross sections are larger at low energies, the ionization energies of the organometallic compounds and the DI thresholds are usually low, within the typical energies of the secondary electrons.

Measuring a complete set of cross sections requires the collaboration of several laboratories and is work-intensive and time-consuming. A serious problem is that a crucial part of the equipment required for such complete cross section measurements, the Maryland instrument for the detection of neutral radicals, existed only once in the world, and is no longer operational.

Many cross sections, those on transient molecules and on excited molecules are hard or impossible to measure and help of theory is indispensable. At the current state theory made a substantial progress in calculating the elastic cross sections, but calculating cross sections for vibrational and electronic excitation is already much more difficult. Methods for calculating the 'chemical' process of DEA *ab initio* for molecules with more than three atoms are just beginning to appear, with the case of acetylene mentioned in sec. III being promising. Calculations of dissociative ionization and neutral dissociation of polyatomic molecules are generally not possible at the present time.

Porting the knowledge from the cross sections to the FEBIP-like conditions poses a number of challenges. The reactive fragments produced in the primary collisions of electrons with the precursor molecule are likely to be involved in further chemical reactions which can only be infered indirectly from the final stable products identified by different surface analytical tools. All the transient chemical species produced are subject to further electron collisions and subsequent chemical change about which we do not have direct information. The primary electron beam is likely to cause local heating, invoking electron collisions with vibrationally excited molecules, the cross sections for which often differ substantially from those for cold molecules, and which are hard to measure.

An important question is whether it is possible to control the outcome of the chemical changes induced by electrons. In DEA attachment there are many cases whether the outcome depends on electron energy, opening the possibility of 'control' in principle. It will be difficult to invoke in reality, however, because it would require the use of quasi-monoenergetic electrons in the 1-15 eV range, which cannot be focussed to sufficiently small spots. The energy-distribution of the electrons is further 'smeared-out' by inelastic collisions in the dense medium.

A second, perhaps more promising approach to 'control' is to design custom precursors where certain cross sections are enhanced and others suppressed. This is possible in some cases - the presence of stable 'leaving groups' like halogens, CO_3^-, or N_2 can enhance DEA cross sections. Local symmetry may also strongly affect DEA cross sections as has been demonstrated with the dihalo-toluenes. The presence of π virtual orbitals leads to pronounced shape resonances and DEA patterns distinctly different from those of saturated compounds.

Acknowledgment

This research is part of the Swiss National Science Foundation project No. 200020-113599/1 and of COST Action CM0601.

[1] L. G. Christophorou and J. K. Olthoff, *Fundamental Electron interactions with Plasma Processing Gases*. New York: Kluwer Academics/Plenum Publishers, 2004.

[2] A. Muñoz, J. C. Oller, F. Blanco, J. D. Gorfinkiel, P. Limão-Vieira, and G. García, "Electron-scattering cross sections and stopping powers in H_2O," *Phys. Rev. A*, vol. 76, no. 5, p. 052707, 2007.

[3] A. Muñoz, J. C. Oller, F. Blanco, J. D. Gorfinkiel, P. Limão-Vieira, and G. García, "Erratum for: Electron-scattering cross sections and stopping powers in H_2O," *Phys. Rev. A*, vol. 76, no. 5, p. 069901, 2007.

[4] A. Muñoz, J. C. Oiler, F. Blanco, J. D. Gorfinkiel, P. Limão-Vieira, A. Maira-Vidal, M. J. G. Borge, O. Tengblad, C. Huerga, M. Téllez, and G. García, "Energy deposition model based on electron scattering cross section data from water molecules," *J. Phys.: Conf. Ser.*, vol. 133, p. 012002, 2008.

[5] N. Silvis-Cividjian and C. W. Hagen, "Electron-beam–induced nanometer-scale deposition," vol. 143, p. 1, 2006.

[6] C. W. Hagen, N. Silvis-Cividjian, and P. Kruit, "Resolution limit for electron beam-induced deposition on thick substrates," *SCANNING*, vol. 28, p. 204, 2006.

[7] C. W. Hagen, W. F. van Dorp, P. Crozier, and P. Kruit, "Electronic pathways in nanostructure fabrication," *Surface Science*, vol. 602, p. 3212, 2008.

[8] M.-W. Ruf, M. Braun, S. Marienfeld, I. I. Fabrikant, and H. Hotop, "High resolution studies of dissociative electron attachment to molecules: dependence on electron and vibrational energy," *J. Phys. Conf. Ser.*, vol. 88, p. 012013, 2007.

[9] H. Kato, M. C. Garcia, T. Asahina, M. Hoshino, C. Makochekanwa, H. Tanaka, F. Blanco, and G. Garcia, "Absolute elastic differential cross sections for electron scattering by $C_6H_5CH_3$ and

$C_6H_5CF_3$ at 1.5–200 eV: A comparative experimental and theoretical study with C_6H_6," *Phys. Rev. A*, vol. 79, p. 062703, 2009.
[10] G. J. Schulz, "Resonances in electron impact on diatomic molecules," *Rev. Mod. Phys.*, vol. 45, p. 423, 1973.
[11] C. Mündel, M. Berman, and W. Domcke, "Nuclear dynamics in resonant electron-molecule scattering beyond the local approximation: Vibrational excitation and dissociative attachment in H_2 and D_2," *Phys. Rev. A*, vol. 32, p. 181.
[12] J. Horáček, M. Čížek, K. Houfek, P. Kolorenč, and W. Domcke, "Dissociative electron attachment and vibrational excitation of H_2 by low-energy electrons: Calculations based on an improved nonlocal resonance model.," *Phys. Rev. A*, vol. 70, p. 052712, 2004.
[13] J. Horáček, M. Čížek, K. Houfek, P. Kolorenč, and W. Domcke, "Dissociative electron attachment and vibrational excitation of H_2 by low-energy electrons: calculations based on an improved nonlocal resonance model. II. vibrational excitation," *Phys. Rev. A*, vol. 73, p. 022701, 2006.
[14] G. J. Schulz and R. K. Asundi, "Isotope effect in the dissociative attachment in H_2 at low energy," *Phys. Rev.*, vol. 158, p. 25, 1967.
[15] B. C. Ibănescu, O. May, A. Monney, and M. Allan, "Electron-induced chemistry of alcohols," *Phys. Chem. Chem. Phys.*, vol. 9, p. 3163, 2007.
[16] O. May, J. Fedor, and M. Allan, "Isotope effect in dissociative electron attachment to acetylene," *Phys. Rev. A*, vol. 80, p. 012706, 2009.
[17] M. Čízek, J. Horáček, M. Allan, I. I. Fabrikant, and W. Domcke, "Vibrational excitation of hydrogen fluoride by low-energy electrons: Theory and experiment," *J. Phys. B*, vol. 36, p. 2837, 2003.
[18] M. Allan, "Selectivity in the excitation of Fermi-coupled vibrations in CO_2 by impact of slow electrons," *Phys. Rev. Lett.*, vol. 87, p. 033201, 2001.
[19] M. Allan, "Vibrational structures in electron-CO_2 scattering below the $^2\Pi_u$ shape resonance," *J. Phys. B: At. Mol. Opt. Phys.*, vol. 35, p. L387, 2002.
[20] H. Hotop, M.-W. Ruf, M. Allan, and I. I. Fabrikant, "Resonance and threshold phenomena in low-energy electron collisions with molecules and clusters," *Adv. At. Mol. Opt. Phys.*, vol. 49, p. 85, 2003.
[21] M. Allan, "Absolute angle-differential elastic and vibrational excitation cross sections for electron collisions with tetrahydrofuran," *J. Phys. B: At. Mol. Opt. Phys.*, vol. 40, p. 3531, 2007.
[22] C. S. Trevisan, A. E. Orel, and T. N. Rescigno, "Elastic scattering of low-energy electrons by tetrahydrofuran," *J. Phys. B: At. Mol. Opt. Phys.*, vol. 39, p. L255, 2006.
[23] C. Winstead and V. McKoy, "Low-energy electron scattering by deoxyribose and related molecules," *J. Chem. Phys.*, vol. 125, p. 074302, 2006.
[24] R. Čurík, P. Čársky, and M. Allan, "Vibrational excitation of methane by slow electrons revisited: Theoretical and experimental study," *J. Phys. B: At. Mol. Opt. Phys.*, vol. 41, p. 115203, 2008.
[25] M. Allan, K. Franz, H. Hotop, O. Zatsarinny, and K. Bartschat, "Absolute angle-differential cross sections for electron-impact excitation of neon within the first 3.5 eV above threshold," *J. Phys. B*, vol. 42, p. 044009, 2009.
[26] M. Allan, C. Winstead, and V. McKoy, "Electron scattering in ethene: excitation of the $\tilde{a}^3B_{1u}$ state, elastic scattering and vibrational excitation," *Phys. Rev. A*, vol. 77, p. 042715, 2008.
[27] Q. Sun, C. Winstead, V. McKoy, and M. A. P. Lima, "Low-energy electron-impact excitation of the $\tilde{a}\ ^3B_{1u}$ ($\pi \rightarrow \pi^*$) state of ethylene," *J. Chem. Phys.*, vol. 96, p. 3531, 1992.
[28] M. Čížek, J. Horáček, A.-C. Sergenton, D. B. Popović, M. Allan, W. Domcke, T. Leininger, and F. X. Gadea, "Inelastic low-energy electron collisions with the HBr and DBr molecules: Experiment and theory," *Phys. Rev. A*, vol. 63, p. 062710, 2001.
[29] J. Fedor, O. May, and M. Allan, "Absolute cross sections for dissociative electron attachment to HCl, HBr, and their deuterated analogs," *Phys. Rev. A*, vol. 78, p. 032701, 2008.
[30] J. Horáček, M. Čížek, P. Kolorenč, and W. Domcke, "Isotope effects in vibrational excitation and dissociative electron attachment of DCl and DBr," *Eur. Phys. J. D*, vol. 35, p. 255, 2005.
[31] R. Abouaf and D. Teillet-Billy, "Fine structure in dissociative-attachment cross sections for hydrogen chloride and deuterium chloride," *J. Phys. B: At. Mol. Phys.*, vol. 10, p. 2261, 1977.
[32] R. Azria and F. Fiquet-Fayard, "Atachment électronique dissociatif sur C_2H_2 et C_2D_2," *J. Physique (Paris)*, vol. 33, p. 663, 1972.
[33] S. T. Chourou and A. E. Orel, "Dissociative attachment to acetylene," *Phys. Rev. A*, vol. 77, no. 4, p. 042709, 2008.
[34] S. T. Chourou and A. E. Orel, "Dissociative attachment to acetylene," *Phys. Rev. A*, p. to be published, 2009.
[35] D. J. Haxton, T. N. Rescigno, and C. W. McCurdy, "Dissociative electron attachment to the H_2O molecule. II. nuclear dynamics on coupled electronic surfaces within the local complex potential model," *Phys. Rev. A*, vol. 75, p. 012711, 2007.
[36] D. J. Haxton, T. N. Rescigno, and C. W. McCurdy, "Erratum," *Phys. Rev. A*, vol. 76, p. 049907, 2007.
[37] S. Ptasińska, S. Denifl, P. Scheier, E. Illenberger, and T. D. Märk, "Bond- and site-selective loss of

H atoms from nucleobases by very-low-energy electrons (<3 eV)," *Angew. Chem. Int. Ed.*, vol. 44, p. 6941, 2005.
[38] V. S. Prabhudesai, A. H. Kelkar, D. Nandi, and E. Krishnakumar, "Functional group dependent site specific fragmentation of molecules by low energy electrons," *Phys. Rev. Lett.*, vol. 95, p. 143202, 2005.
[39] B. C. Ibanescu and M. Allan, "A dramatic difference between the electron-driven dissociation of alcohols and ethers and its relation to Rydberg states," *Phys. Chem. Chem. Phys.*, vol. 10, p. 5232, 2008.
[40] B. C. Ibanescu and M. Allan, "Selective cleavage of the C-O bonds in alcohols and asymmetric ethers by dissociative electron attachment," *Phys. Chem. Chem. Phys.*, p. at press, 2009.
[41] R. Dressler, M. Allan, and E. Haselbach, "Symmetry control in bond cleavage processes: Dissociative electron attachment to unsaturated halocarbons," *Chimia*, vol. 39, p. 385, 1985.
[42] K. L. Stricklett, S. C. Chu, and P. D. Burrow, "Dissociative attachment in vinyl and allyl chloride, chlorobenzene and benzyl chloride," *Chem. Phys. Lett.*, vol. 131, p. 279, 1986.
[43] C. Bulliard, M. Allan, and E. Haselbach, "Intramolecular competition of phenylic and benzylic CX bond breaking in dissociative electron attachment to dihalotoluenes," *J. Phys. Chem.*, vol. 98, p. 11040, 1994.
[44] C. Bulliard, M. Allan, and S. Grimme, "Electron energy loss and dissociative electron attachment spectroscopy of methyl vinyl ether and related compounds," *Int. J. of Mass Spectr. and Ion Proc.*, vol. 205, p. 43, 2001.
[45] S. Živanov, B. C. Ibănescu, M. Paech, M. Poffet, P. Baettig, A.-C. Sergenton, S. Grimme, and M. Allan, "Dissociative electron attachment and electron energy loss spectra of phenyl azide," *J. Phys. B: At. Mol. Opt. Phys.*, vol. 40, p. 101, 2007.
[46] M. A. Lieberman and A. J. Lichtenberg, *Principles of Plasma Discharges and Materials Processing*. New York: John Wiley & Sons, 1994.
[47] I. Shimamura and K. Takayanagi, eds., *Electron-Molecule Collisions*. New York: Plenum Press, 1984.
[48] A. Gilardini, *Low Energy Electron Collisions in Gases*. New York: John Wiley & Sons, 1972.
[49] W. Hack, "Detection methods for atoms and radicals in the gas phase," *International Reviews in Physical Chemistry*, vol. 4, 1985.
[50] E. Paneth and W. Hofeditz, "Preparation of free methyl," *Ber. Dt. Chem. Ges. B*, vol. 62, p. 1335, 1929.
[51] F. O. Rice and M. D. Dooley, "Thermal decomposition of organic compounds from the standpoint of free radicals. XII. the decomposition of methane," *J. Am. Chem. Soc.*, vol. 56, p. 2747, 1934.
[52] L. Belchetz and E. Rideal, "The primary decomposition of hydrocarbon vapors on carbon filaments," *J. Am. Chem. Soc.*, vol. 57, p. 1168, 1935.
[53] S. J. B. Corrigan, "Dissociation of molecular hydrogen by electron impact," *J. Chem. Phys.*, vol. 43, p. 4381, 1965.
[54] H. F. Winters and M. Inokuti, "Total dissociation cross section of tetrafluoromethane and other fluoroalkanes for electron impact," *Phys. Rev. A*, vol. 25, p. 1420, 1982.
[55] Y. Ohmori, K. Kitamori, M. Shimozuma, and H. Tagashira, "Boltzmann equation analysis of electron swarm behavior in methane," *J. Phys. D*, vol. 19, p. 437, 1986.
[56] Y. Nakamura, *Gaseous Electronics and Their Applications*, p. 178. Tokyo, Japan: KTK Scientific, 1991.
[57] W. L. Morgan, "A critical evaluation of low-energy electron impact cross sections for plasma processing modeling. II: tetrafluoromethane, silane, and methane," *Plasma Chem. Plasma Proc.*, vol. 12, 1992.
[58] M. Hayashi, *Swarm Studies and Inelastic Electron-Molecule Collisions*, p. 167. New York: Springer, 1987.
[59] R. A. Bonham, "Electron impact cross section data for carbon tetrafluoride," *Jpn. J. Appl. Phys. 1*, vol. 33, 1994.
[60] D. K. Davies, L. E. Kline, and W. E. Bies, "Measurements of swarm parameters and derived electron collision cross sections in methane," *J. Appl. Phys.*, vol. 65, 1989.
[61] F. J. de Heer, "Electron excitation, dissociation and ionization of hydrogen, deuterium and tritium molecules, simple hydrocarbons and their ions," *Phys. Scr.*, vol. 23, p. 170, 1981.
[62] S. Motlagh and J. H. Moore, "Cross sections for radicals from electron impact on methane and fluoroalkanes," *J. Chem. Phys.*, vol. 109, p. 432, 1998.
[63] L. Mi and R. A. Bonham, "Electron-ion coincidence measurements: the neutral dissociation cross section for CF_4," *J. Chem. Phys.*, vol. 108, p. 1910, 1998.
[64] H. Tanaka, H. Toyda, and H. Sugai, "Cross sections for electron-impact dissociation of alternative etching gas, C_3HF_7O," *Jpn. J. Appl. Phys.*, vol. 37, p. 5053, 1998.
[65] J. Perrin, J. P. M. Schmitt, G. D. Rosny, B. Drevillon, J. Huc, and A. Lloret, "Dissociation cross sections of silane and disilane by electron impact," *Chem. Phys.*, vol. 73, p. 383, 1982.
[66] H. C. Straub, D. Lin, B. G. Lindsay, K. A. Smith, and R. F. Stebbings, "Absolute partial cross sections for electron-impact ionization of CH_4 from threshold to 1000 eV," *J. Chem. Phys.*, vol. 106,

1997.
[67] H. F. Winters, "Dissociation of methane by electron impact," *J. Chem. Phys.*, vol. 63, p. 3462, 1975.
[68] M. Goto, K. Nakamura, H. Toyoda, and H. Sugai, "Cross section measurements for electron-impact dissociation of CHF_3 into neutral and ionic radicals," *Jpn. J. Appl. Phys., Pt. 1*, vol. 33, 1994.
[69] J. E. Baio, H. Yu, D. W. Flaherty, H. F. Winters, and D. B. Graves, "Electron-impact dissociation cross sections for CHF_3 and C_3F_8," *J. Phys, D: Appl. Phys.*, vol. 40, p. 6969, 2007.
[70] H. Toyoda, M. Ito, and H. Sugai, "Cross section measurements for electron-impact dissociation of C_4F_8 into neutral and ionic radicals," *Jpn. J. Appl. Phys.*, vol. 36, p. 3730, 1997.
[71] L. G. Christophorou, J. K. Olthoff, and M. V. V. S. Rao, "Electron interactions with CF_4," *J. Phys. Chem. Ref. Data*, vol. 25, 1996.
[72] L. G. Christophorou, J. K. Olthoff, and M. V. V. S. Rao, "Electron interactions with CHF_3," *J. Phys. Chem. Ref. Data*, vol. 26, 1997.
[73] L. G. Christophorou and J. K. Olthoff, "Electron interactions with C_2F_6," *J. Phys. Chem. Ref. Data*, vol. 27, 1998.
[74] T. Shirai, T. Tabata, H. Tawara, and Y. Itikawa, "Analytic cross sections for electron collisions with hydrocarbons: CH_4, C_2H_6, C_2H_4, C_2H_2, C_3H_8, and C_3H_6," *At. Data Nucl. Data Tables*, vol. 80, p. 147, 2002.
[75] C. Ma, M. R. Bruce, and R. A. Bonham, "Absolute partial and total electron-impact-ionization cross sections for tetrafluoromethane from threshold up to 500 eV," *Phys. Rev. A*, vol. 44, p. 2921, 1991.
[76] C. Ma, M. R. Bruce, and R. A. Bonham, "Erratum," *Phys. Rev. A*, vol. 45, p. 6932, 1992.
[77] R. A. Bonham, "Electron impact cross section data for carbon tetrafluoride," *Jpn. J. Appl. Phys. 1*, vol. 33, p. 4157, 1994.
[78] H. U. Poll, C. Winkler, D. Margreiter, V. Grill, and T. D. Märk, "Discrimination effects for ions with high initial kinetic energy in a Nier-type ion source and partial and total electron ionization cross-sections of carbon tetrafluoride," *Int. J. Mass Spectrom. Ion Processes*, vol. 112, p. 1, 1992.
[79] M. R. Bruce, C. Ma, and R. A. Bonham, "Electron impact cross section data for carbon tetrafluoride," *Chem. Phys. Lett.*, vol. 190, p. 285, 1992.
[80] T. D. Märk, *Electron-Molecule Interactions and Their Applications*. Orlando: Academic Press, 1984.
[81] T. D. Märk and G. H. Dunn, *Electron Impact Ionisation*. Springer-Verlag, 1985.
[82] E. W. McDaniel, *Atomic Collisions, Electron and Photon Projectiles*. New York: John Wiley & Sons, 1986.
[83] E. Illenberger and J. Momigny, eds., *Gaseous Molecular Ions*. New York: Steinkopf Verlag Darmstadt/Springer Verlag, 1992.
[84] K. H. Becker and V. Tarnovsky, "Electron-impact ionization of atoms, molecules, ions and transient species," *Plasma Sources Sci. Technol.*, vol. 4, p. 307, 1995.
[85] in *NIST Chemistry WebBook, NIST Standard Reference Database Number 69* (P. J. Linstrom and W. G. Mallard, eds.), http://webbook.nist.gov, retrieved July 21, 2009.
[86] F. W. McLafferty and F. Tureček, *Interpretation of mass spectra, 4th edition*, p. 55. University Science books, 1993.
[87] J. Lango, L. Szepes, P. Csaszar, and G. Inorta, "Studies on the unimolecular decomposition of organometallic ions," *J. Organometal. Chem.*, vol. 269, p. 133, 1984.
[88] H. Deutsch, D. Margreiter, and T. D. Märk, "Total electron impact ionization cross-sections of free molecular radicals: a case of failure of the additivity rule?," *Int. J. Mass Spectrom Ion Proc.*, vol. 93, p. 259, 1989.
[89] H. Deutsch, T. D. Märk, V. Tamovsky, K. Becker, C. Comelissen, L. Cespive, and V. Bonacic-Koutecky, "Measured and calculated absolute total cross-sections for the single ionization of CF_x and NF_x by electron impact," *Int. J. Mass Spect. Ion Proc.*, vol. 137, p. 77, 1994.
[90] T. D. Märk, "Ionization by electron impact," *Plasma Phys. Control. Fusion*, vol. 34, p. 2083, 1992.
[91] Y. K. Kim and M. E. Rudd, "Binary-encouter-dipole model for electron-impact ionization," *Phys. Rev. A*, vol. 50, p. 3954, 1994.
[92] S. J. King and S. D. Price, "Electron ionization of H_2O," *Int. J. Mass Spect.*, vol. 277, p. 84, 2008.
[93] C. Tian and C. R. Vidal, "Electron impact dissociative ionization of CO_2: Measurements with a focusing time-of-flight mass spectrometer," *J. Chem. Phys.*, vol. 108, p. 927, 1998.
[94] R. Basner, M. Schmidt, and K. Becker, "Absolute total and partial cross sections for the electron impact ionization of diborane (B_2H_6)," *J. Chem. Phys.*, vol. 118, p. 2153, 2003.
[95] K. Gluch, P. Scheier, W. Schustereder, T. Tepnual, L. Feketeova, C. Mair, S. Matt-Leubner, A. Stamatovic, and T. D. Märk, "Cross sections and ion kinetic energies for electron impact ionization of CH_4," *Int. J. Mass Spect.*, vol. 228, p. 307, 2003.
[96] M. A. Mangan, B. G. Lindsay, and R. F. Stebbings, "Absolute partial cross sections for electron-impact ionization of CO from threshold to 1000 eV," *J. Phys. B: At. Mol. Opt. Phys.*, vol. 33, p. 3225, 2000.
[97] R. E. Winters and R. W. Kiser, "Ionization and fragmentation of dimethylzinc, trimethylaluminum, and trimethylantimony," *J. Organometal. Chem.*, vol. 10, p. 7, 1967.
[98] C. Q. Jiao, C. A. DeJoseph Jr., P. Haaland, and A. Garscadden, "Electron impact ionization and

ion chemistry in trimethylaluminum and in trimethylgallium," *Int. J. Mass Spectr.*, vol. 202, p. 345, 2000.

[99] F. Glockling and R. G. Strafford, "Electron impact studies on some group III metal alkyls," *J. Chem. Soc. A*, p. 1761, 1971.

[100] J. Opitz, "Electron impact ionization of cobalt-tricarbonyl-nitrosyl, cyclopentadienyl-cobalt-dicarbonyl and biscyclopentadienyl-cobalt: appearance energies, bond energies and enthalpies of formation," *Int. J. Mass Spectr.*, vol. 225, p. 115, 2003.

[101] J. F. Nixon, R. J. Suffolk, M. J. Taylor, J. G. Norman Jr., D. E. Hoskins, and D. J. Gmur, "Photoelectron and electronic spectra of $Rh_2Cl_2(CO)_4$ and $Rh_2Cl_2(PF_3)_4$: Assignments from SCF-Xa-SW calculations," *Inorg. Chem.*, vol. 19, p. 810, 1980.

[102] G. D. Michels and H. J. Svec, "Characterization of $MnTc(CO)_{10}$ and $TcRe(CO)_{10}$," *Inorg. Chem.*, vol. 20, p. 3445, 1981.

[103] S. Barfuss, K. H. Emrich, W. Hirschwald, P. A. Dowben, and N. M. Boag, "A mass spectrometric investigation of chloro-, bromo- and methylferrocenes by electron and photon impact ionization," *J. Organomet. Chem.*, vol. 391, p. 209, 1990.

[104] E. Vasekova, M. Stano, S. Matejcik, J. D. Skalný, P. Mach, T. D. Märk, and J. Urban, "Electron impact ionization of C_2H_6: ionization energies and temperature effects," *Int. J. of Mass Spect.*, vol. 235, p. 155, 2004.

[105] S. Denifl, S. Matejcik, J. D. Skalný, M. Stano, P. Mach, J. Urban, P. Scheier, T. D. Märk, and W. Barszczewska, "Electron impact ionization of C_3H_8: appearance energies and temperature effects," *Chem. Phys. Lett.*, vol. 402, p. 80, 2005.

[106] A. Popovic, "Mass spectrometric determination of the ionisation cross-sections of BaO, Ba, BaF_2 and BaI_2 by electron impact," *Int. J. Mass Spect.*, vol. 230, p. 99, 2003.

[107] R. Basner, M. Schmidt, and H. Deutsch, "Electron impact ionization and fragmentation of metal-organic compounds used in plasma assisted thin film deposition techniques," *Contrib. Plasma Phys.*, vol. 35, p. 375, 1995.

[108] D. Bruch, J. Opitz, and G. von Bünau, "Electron impact and multiphoton ionization and fragmentation of molybdenum-cyclopentadienyl-dicarbonyl-nitrosyl at 351, 248 and 193 nm," *Int. J.Mass Spect. Ion Proc.*, vol. 171, p. 147, 1997.

[109] S. Barfuss, M. Grade, W. Hirschwald, W. Rosinger, N. M. Boag, D. C. Driscoll, and P. A. Dowben, "The stability and decomposition of gaseous chloroferrocenes," *J. Vac. Sci. Technol. A*, vol. 5, p. 1451, 1987.

[110] V. H. Dibeler, "Mass spectra of the tetramethyl compounds of carbon silicon, germanium, tin, and lead," *J. Research NBS*, vol. 49, p. 235, 1952.

[111] R. B. King, "Mass spectra of organometallic compounds. VI. some indenylmetal derivatives and related compounds," *Can. J. Chem.*, vol. 47, p. 559, 1969.

[112] A. Bjarnason, "Fourier transform mass spectrometry of several organometallic complexes: Laser desorption versus electron impact ionization," *Oganometallics*, vol. 9, p. 657, 1990.

[113] M. N. Rocklein and D. P. Land, "Mass spectra of $Fe(CO)_5$ using Fourier transform mass spectrometry (FTMS) and laser induced thermal desorption FTMS with electron ionization, charge exchange, and proton transfer," *Int. J.Mass Spect.*, vol. 177, p. 83, 1998.

[114] S. Georgiou, E. Mastoraki, E. Raptakis, and Z. Xenidi, "The potential of VUV photoionisation mass spectrometry in monitoring photofragmentation of organometallics," *Laser Chem.*, vol. 13, p. 113, 1993.

[115] P. J. Bassett, B. R. Higginson, D. R. Lloyd, N. Lynaugh, and P. J. Roberts, "Helium-I photoelectron spectra of tetrakis(trifluoro-phosphine)-nickel(0), -palladium(0), and -platinum(0)," *J. Chem. Soc. Dalton Trans.*, vol. 21, p. 2316, 1974.

[116] D. S. Yang, G. M. Bancroft, R. J. Puddephatt, K. H. Tan, J. N. Cutler, and J. D. Bozek, "Assignment of the valence molecular orbitals of $CpPtMe_3$ and $Me_2Pt(COD)$ using variable-energy photoelectron spectra," *Inorg. Chem.*, vol. 29, p. 4956, 1990.

[117] P. Seuret, F. Cicoira, T. Ohta, P. Doppelt, P. Hoffmann, J. Weber, and T. A. Wesolowski, "An experimental and theoretical study of $[RhCl(PF_3)_2]_2$ fragmentation," *Phys. Chem. Chem. Phys.*, vol. 5, p. 268, 2003.

[118] M. Polášek and J. Kubišta, "Bis(eta^5-cyclopentadienyl)titanium(II) in the gas phase: Mass spectrometric and computational study of the structure and reactivity," *J. Organomet. Chem.*, vol. 692, p. 4073, 2007.

[119] R. B. Sohnlein and D.-S. Yanga, "Pulsed-field ionization electron spectroscopy of group 6 metal Cr, Mo, and W bis benzene sandwich complexes," *J. Chem. Phys.*, vol. 124, p. 134305, 2006.

[120] F. Qi, S. Yang, L. Sheng, H. Gao, Y. Zhang, and S. Yu, "Vacuum ultraviolet photoionization and dissociative photoionization of $W(CO)_6$," *J. Chem. Phys.*, vol. 107, p. 10391, 1997.

[121] B. Samorski, J. M. Hosenlopp, D. Rooney, and J. Cheiken, "The effect of deuteration on multiphoton dissociation of benzene chromium tricarbonyl," *J. Chem. Phys.*, vol. 85, p. 3326, 1986.

[122] P. B. Armentrout and J. L. Beauchamp, "The chemistry of atomic transition-metal ions: Insight into fundamental aspects of organometallic chemistry," *Acc. Chem. Res.*, vol. 22, p. 315, 1989.

[123] I. Ipolyi, W. Michaelis, and P. Swiderek, "Electron-induced reactions in condensed films of acetonitrile and ethane," *Phys. Chem. Chem. Phys.*, vol. 8, p. 180, 2007.
[124] D. R. Lide, *CRC Handbook of Chemistry and Physics. 86th Edition.* Taylor & Francis, 2005.
[125] M. Tronc, R. Azria, Y. L. Coat, and E.Illenberger, "Threefold differential electron-stimulated desorption yields of D^- anions from multilayer films of D_2O and ND_3 condensed on platinum," *J. Phys. Chem.*, vol. 100, p. 14745, 1996.
[126] L. Sanche, "Electron resonances in DIET," *Surf. Sci.*, vol. 451, p. 82, 2000.
[127] M. A. Huels, P.-C. Dugal, and L. Sanche, "Degradation of functionalized alkanethiolate monolayers by 0-18 eV electrons," *J. Chem. Phys.*, vol. 118, p. 11168, 2003.
[128] J. D. Wnuk, J. M. Gorham, S. Rosenberg, W. F. van Dorp, T. E. Madey, C. W. Hagen, and D. H. Fairbrother, "Electron induced surface reactions of the organometallic precursor trimethyl(methylcyclopentadienyl)platinum(IV)," *J. Phys. Chem. C*, vol. 113, p. 2487, 2009.
[129] T. D. Harris, D. H. Lee, M. Q. Blumberg, and C. R. Arumainayagam, "Electron-induced reactions in methanol ultrathin films studied by temperature-programmed desorption: A useful method to study radiation chemistry," *J. Phys. Chem.*, vol. 99, p. 9530, 1995.
[130] W. Eck, V. Stadler, W. Geyer, M. Zharnikov, A. Gölzhäuser, and M. Grunze, "Generation of surface amino groups on aromatic self-assembled monolayers by low energy electron beams - a first step towards chemical lithography," *Adv. Mater.*, vol. 12, p. 805, 2000.
[131] M. Lepage, M. Michaud, and L. Sanche, "Low-energy electron scattering cross section for the production of CO within condensed acetone," *J. Chem. Phys.*, vol. 113, p. 3602, 2000.
[132] C. Jäggle, P. Swiderek, S.-P. Breton, M. Michaud, and L. Sanche, "Products and reaction sequences in tetrahydrofuran exposed to low-energy electrons," *J. Phys. Chem. B*, vol. 110, p. 12512, 2006.
[133] C. Olsen and A. Rowntree, "Bond-selective dissociation of alkanethiol based self-assembled monolayers adsorbed on gold substrates, using low-energy electron beams," *J. Chem. Phys.*, vol. 108, p. 3750, 1998.
[134] L. Sanche, "Transmission of 0-15 eV monoenergetic electrons through thin-film molecular solids," *J. Chem. Phys.*, vol. 71, p. 4860, 1979.
[135] M. N. Hedhili, J. H. Bredehöft, and P. Swiderek, "Electron-induced reactions of $MeCpPtMe_3$ investigated by HREELS," *J. Phys. Chem. C*, vol. 113, p. 13282, 2009.
[136] R. L. Graham, C. D. Bain, H. A. Biebuyck, E. Laibinis, and G. M. Whitesides, "Damage to CF_3CONH-terminated organic self-assembled monolayers (SAMs) on Al, Ti, Cu, and Au by Al Kα X-rays is due principally to electrons," *J. Phys. Chem.*, vol. 97, p. 9456, 1993.
[137] E. Burean, I. Ipolyi, T. Hamann, and P. Swiderek, "Thermal desorption spectrometry for the study of electron-induced reactions," *Int. J. Mass Spectrom.*, vol. 277, p. 215, 2008.
[138] P. Swiderek, C. Jäggle, D. Bankmann, and E. Burean, "Fate of reactive intermediates formed in acetaldehyde under exposure to low-energy electrons," *J. Phys. Chem. C*, vol. 111, p. 303, 2007.
[139] E. Burean and P. Swiderek, "Electron-induced reactions in condensed acetaldehyde: Identification of products and energy dependent cross sections," *J. Phys. Chem. C*, vol. 112, p. 19456, 2008.
[140] J. R. Swanson, F. A. Flitsch, and C. M. Friend, "Low energy electron induced decomposition on surfaces: $W(CO)_6$ on Si(111)-(7×7)," *Surf. Sci.*, vol. 215, p. L293, 1989.
[141] K. Svensson, T. R. Bedson, and R. E. Palmer, "Dissociation and desorption of ferrocene on graphite by low energy electron impact," *Surf. Sci.*, vol. 451, p. 250, 2000.
[142] Y. Wang, F. Gao, M. Kaltchev, and W. T. Tysoe, "The effect of electron beam irradiation on the chemistry of molybdenum hexacarbonyl on thin alumina films in ultrahigh vacuum," *J. Mol. Catal. A*, vol. 209, p. 135, 2004.
[143] L. Sanche, "Effects of the solid phase on resonance stabilization, dissociative attachment and dipolar dissociation," in *Linking the gaseous and condensed phases of matter* (L. G. Christophorou, E. Illenberger, and W.-F. Schmidt, eds.), p. 377, Plenum Press, New York, 1994.
[144] A. Bass and L. Sanche, "Absolute and effective cross-sections for low-energy electron-scattering processes within condensed matter," *Radiat. Environ. Biophysics*, vol. 37, p. 243, 1998.
[145] I. Bald, J. Langer, P. Tegeder, and O. Ingólfsson, "From isolated molecules through clusters and condensates to the building blocks of life - A short tribute to Prof. Eugen Illenbergers work in the field of negative ion chemistry," *Int. J. Mass Spectrom.*, vol. 277, p. 4, 2008.
[146] W. Sailer, A. Pelc, P. Limão-Vieira, N. J. Mason, J. Limtrakul, and T. D. M. P. Scheier, M. Probst, "Low energy electron attachment to CH_3CN," *Chem. Phys. Lett.*, vol. 381, p. 216, 2003.
[147] T. Hamann, J. H. Bredehöft, and P. Swiderek p. manuscript under preparation.
[148] T. Hamann, E. Böhler, and P. Swiderek, "Low-energy electron-induced hydroamination of an alkene," *Angew. Chem. Int. Ed.*, vol. 48, p. 4643, 2009.
[149] I. Ipolyi, E. Burean, T. Hamann, M. Cingel, S. Matejcik, and P. Swiderek, "Low-energy electron-induced chemistry of condensed-phase hexamethyldisiloxane: Initiating dissociative process and subsequent reactions," *Int. J. Mass Spectrom.*, vol. 282, p. 133, 2009.
[150] X. Pan, A. D. Bass, J. Jay-Gerin, and L. Sanche, "A mechanism for the production of hydrogen peroxide and the hydroperoxyl radical on icy satellites by low-energy electrons," *Icarus*, vol. 172, p. 521, 2004.

[151] A. Lafosse, M. Bertin, A. Domaracka, D. Pliszka, E. Illenberger, and R. Azria, "Reactivity induced at 25 K by low-energy electron irradiation of condensed NH_3-CH_3COOD (1:1) mixture," *Phys. Chem. Chem. Phys.*, vol. 8, p. 5564, 2006.

[152] N. Nakayama, E. E. Ferrenz, D. R. Ostling, A. S. Nichols, J. F. Faulk, and C. R. Arumainayagam, "Surface chemistry and radiation chemistry of trifluoroiodomethane (CF_3I) on Mo(110)," *J. Phys. Chem. B*, vol. 108, p. 4080, 2004.

[153] L. D. Weeks, L. L. Zhu, M. Pellon, D. R. Haines, and C. R. Arumainayagam, "Low-energy electron-induced oligomerization of condensed carbontetrachloride," *J. Phys. Chem. C*, vol. 111, p. 4815, 2007.

[154] E. Burean and P. Swiderek, "Thermal desorption measurements of cross-sections for reactions in condensed acetaldehyde induced by low-energy electrons," *Surf. Sci.*, vol. 602, p. 3194, 2008.

[155] E. Burean, I. Ipolyi, T. Hamann, and P. Swiderek, "Thermal desorption spectrometry for the identification of products formed by electron-induced reactions," *Int. J. Mass Spectrom.*, vol. 277, p. 215, 2008.

[156] "Nature abhors a vacuum ... and She's none too fond of an unpaired electron either." Anonymous